

Department of Biomedical Sciences
University of Veterinary Medicine Vienna
Institute of Pharmacology and Toxicology
Head: Univ. Prof. Dr. Veronika Sexl

**Glycolytic vs. mitochondrial function of
Leishmania tarentolae promastigotes**

Bachelor thesis submitted for the fulfilment of the requirements for the degree of

Bachelor of Science (BSc.)

University of Veterinary Medicine Vienna

submitted by

Anja Maria Holzer

Vienna, May 2021

Supervisor: Ao. Univ. Prof. Dr. Katrin Staniek

University of Veterinary Medicine Vienna
Department of Biomedical Sciences
Institute of Pharmacology and Toxicology
Veterinärplatz 1
1210 Vienna

Reviewer: Dipl.-Biol. Dr. rer. nat. Rudolf Moldzio

University of Veterinary Medicine Vienna
Department of Biomedical Sciences
Institute of Medical Biochemistry
Veterinärplatz 1
1210 Vienna

TABLE OF CONTENT

1	Introduction	1
1.1	<i>Leishmania</i>	1
1.2	Metabolism of <i>Leishmania</i> promastigotes and amastigotes.....	2
1.3	Inhibitors of metabolism.....	5
1.4	Aims of the study	6
2	Materials and Methods.....	7
2.1	Chemicals.....	7
2.2	Cell culture of <i>Leishmania tarentolae</i> promastigote	9
2.3	Determination of cell number.....	9
2.4	Determination of protein concentration.....	10
2.5	Determination of oxygen consumption rates using OxoPlates®	11
2.5.1	Measurement principle of the OxoPlates® OP96U	11
2.5.2	Calibration of OxoPlates® OP96U	11
2.5.3	Determination of oxygen consumption rates of <i>Leishmania tarentolae</i> promastigotes	12
2.6	Determination of extracellular acidification rates using HydroPlates®	12
2.6.1	Measurement principle of the HydroPlates® HP96U	12
2.6.2	Calibration of HydroPlates® HP96U.....	13
2.6.3	Determination of extracellular acidification rates of <i>Leishmania tarentolae</i> promastigotes	14
2.7	Data analysis and statistics	14
3	Results	15
3.1	Protein content of <i>Leishmania tarentolae</i> promastigotes	15
3.2	Determination of buffer factor	15
3.3	Oxygen consumption and extracellular acidification rates of <i>Leishmania tarentolae</i> promastigotes in the presence of mitochondrial inhibitors.....	16

3.3.1	Mitochondrial complex I inhibitor rotenone	16
3.3.2	Mitochondrial complex III inhibitors antimycin A and myxothiazol	18
3.4	Oxygen consumption and extracellular acidification rates of <i>Leishmania tarentolae</i> promastigotes in the presence of an ATP synthase inhibitor and an uncoupler	24
3.5	Mitochondrial bioenergetic vs. glycolytic activity of <i>Leishmania tarentolae</i> promastigotes	26
3.6	Oxygen consumption and extracellular acidification rates of <i>Leishmania tarentolae</i> promastigotes in the presence of an inhibitor of glycolysis	28
3.7	Mitochondrial bioenergetic vs. glycolytic activity of <i>Leishmania tarentolae</i> promastigotes in the presence of different mitochondrial inhibitors and an inhibitor of glycolysis	30
4	Discussion	32
5	Summary	35
6	Zusammenfassung	36
7	List of Abbreviations	37
8	List of Figures	38
9	References	41
10	Acknowledgements	44

1 INTRODUCTION

1.1 *Leishmania*

The members of the genus *Leishmania* are protozoan parasites transmitted by the bite of sandflies (Kaye and Scott 2011). *Leishmania* spp. belong to the family *Trypanosomatidae*. They are the cause of a lot of different infectious diseases like Chagas disease, sleeping sickness and leishmaniasis (Fidalgo and Gille 2011). The latter one poses a danger to over 350 million people in 88 different countries around the world. The infection can be caused by one of several different species of the genus *Leishmania* (Kaye and Scott 2011).

Different species of *Leishmania* induce different forms of leishmaniasis. *L. donovani* and *L. infantum* manifest in form of visceral leishmaniasis, which is the cause for over 70,000 deaths per year. In contrast, *L. major*, *L. tropica* and *L. amazonensis* are examples for parasites that initiate cutaneous leishmaniasis. There is also a third disease manifestation in form of the mucocutaneous leishmaniasis that is caused by pathogens like *L. braziliensis* (Kaye and Scott 2011).

Leishmania tarentolae were first isolated from geckos of the species *Tarentola mauritanica* in 1921. Unlike the other species mentioned above, they are not pathogenic to humans. Thus, they can be easily used in experimental setups representing other *Leishmania* species as a model system (Klatt et al. 2019). *Leishmania tarentolae* therefore are categorized as biosafety level 1 pathogens (Taylor et al. 2010).

The life cycle of *Leishmania* parasites is maintained through transmission between insects (sandfly) and mammalian hosts (Figure 1). The habitat of promastigotes, the motile, flagellated form of *Leishmania* spp., is the midgut of sandflies. In these vectors they go through different morphological stages of differentiation and proliferation to become infectious. During the sandfly bite, infectious promastigotes are transmitted to the mammalian host. After entering the mammalian host, the promastigotes are subsequently phagocytosed by various possible cell types of various tissues. They create an intracellular residence in a predominantly acidic surrounding in the phagolysosome (Kaye and Scott 2011). Thus, the promastigotes start their differentiation into amastigotes. This process involves changes in gene expression (Rosenzweig et al. 2008, Kaye and Scott 2011). Amastigotes are the aflagellated form of *Leishmania* spp. and predominantly occur as intracellular parasites in macrophages. They replicate inside the host cell, until they rupture the cell. The so released amastigotes are able to reinfect other cells in the surroundings.

When an infected cell gets taken up by a sandfly through a bite, the transmission cycle is complete. Amastigotes can then convert into promastigotes again and restart the life cycle of *Leishmania* (Kaye and Scott 2011).

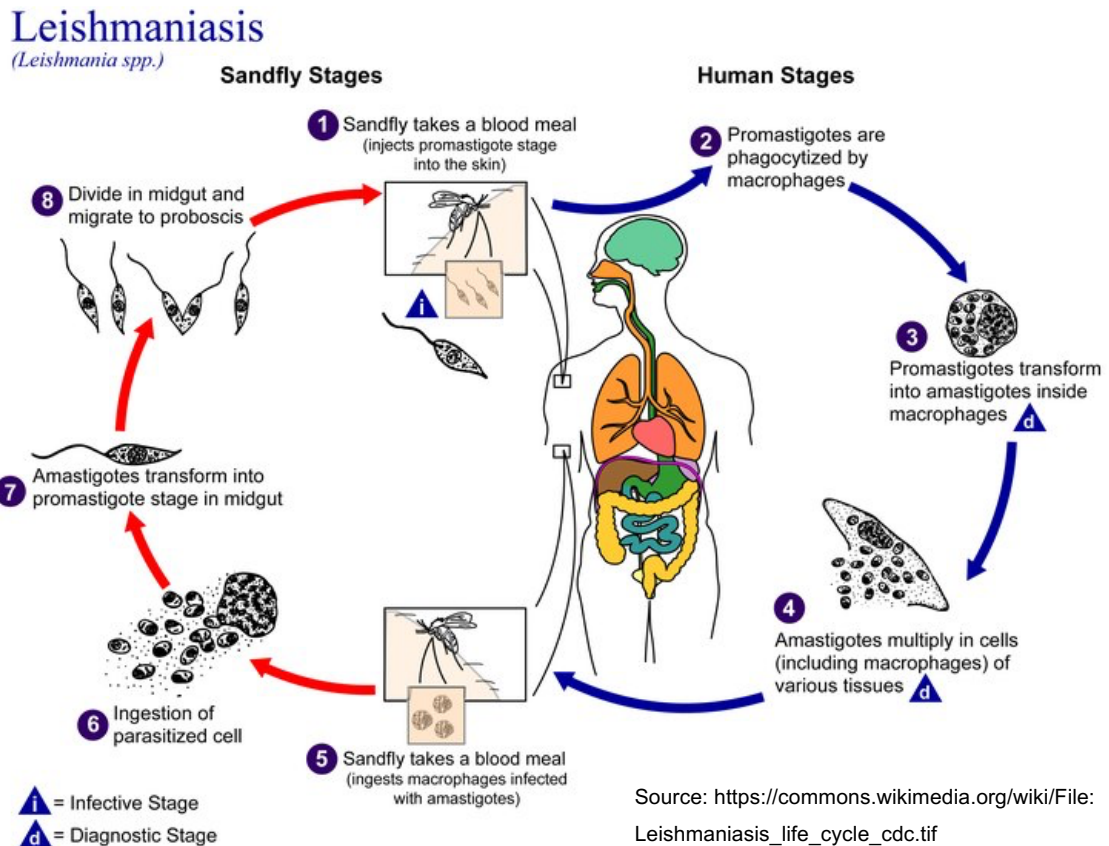


Figure 1: Life cycle of the genus *Leishmania*

1.2 Metabolism of *Leishmania* promastigotes and amastigotes

These extremely different environments require metabolic modifications of the *Leishmania* parasites to match the nutrient availability in each form (Burchmore and Hart 1995). They need highly adaptable metabolic and physiological systems to survive. The habitat of extracellular promastigotes is the alimentary tract of sandflies, surroundings that are rich in glucose and other carbohydrates and are slightly alkaline. Whereas the intracellular amastigotes are confronted with an acidic milieu, containing poor glucose amounts but a high abundance of amino acids.

During differentiation from promastigotes to amastigotes, *Leishmania* undergo a shift from glucose to fatty acids and amino acids as their main source of energy. The two forms are adapted to their optimal pH each. Promastigotes carry out activities like respiration, catabolism of energy substrates and synthesis of macromolecules at neutral pH. Whereas amastigotes perform these at acidic pH. In promastigotes glycolysis is more active than in amastigotes, where fatty acid oxidation and gluconeogenesis are the predominant metabolic pathways. The activity of mitochondrial respiration increases during differentiation from promastigotes to amastigotes. Furthermore, proteins of oxidative phosphorylation, enzymes involved in the citric acid cycle and the mitochondrial respiratory chain are up regulated in the amastigote form. Thus, amastigotes seem to be perfectly adapted to their habitat in the phagolysosome, with less carbohydrates, but a lot of amino acids, phospholipids, triglycerides, and fatty acids (Rosenzweig et al. 2008). Nonetheless, it was recently shown that although amastigotes can use amino acids as major carbon sources in non-activated macrophages, they appear to be highly dependent on sugars as their major carbon source for their intracellular survival in activated macrophages (Saunders et al. 2018).

In addition, the mitochondrial bioenergetic functions seem to be different between the amastigote and promastigote stages (Mondal et al. 2014). *Leishmania* parasites have only one large mitochondrion, that is ramified. It provides the majority of the parasite's energy requirement (Kathuria et al. 2014). The single mitochondrion of *Leishmania* takes up around 12 % of the whole cell volume. It is also associated with the kinetoplast to form a kinetoplast-mitochondrial complex (Chakraborty et al. 2010).

The main role of mitochondria is adenosine triphosphate (ATP) synthesis enabled by the respiratory chain and oxidative phosphorylation. There are five multi-subunit complexes (I-V) embedded in the mitochondrial inner membrane that are associated with ATP synthesis (Figure 2). In the cell, carbohydrates are oxidized by glycolysis and fatty acids are oxidized by β -oxidation, both processes finally resulting in acetyl coenzyme A. The latter is further metabolized in the citric acid cycle, where nicotinamide adenine dinucleotide (NAD^+) is reduced to NADH. NADH is then oxidized to NAD^+ at complex I in the respiratory chain (NADH:ubiquinone oxidoreductase), while the electrons of complex I are transmitted to coenzyme Q (ubiquinone). In addition, electrons can be transferred to ubiquinone via complex II (succinate:ubiquinone oxidoreductase). The electrons then are transported through complex III (ubiquinol:cytochrome c oxidoreductase) to cytochrome c and finally to complex IV (cytochrome c oxidase). At complex IV the electrons are used to reduce oxygen to water.

The redox energy released by the respiratory chain (complex I-IV) is used to pump protons out of the matrix and build up a proton gradient across the inner mitochondrial membrane. If adenosine diphosphate (ADP) is available, the gradient causes protons to flow back through complex V (F_0F_1 -ATP synthase) where ATP is synthesized from ADP and phosphate (Smith et al. 2012).

One of many methodologies for analysing the mitochondrial oxidative phosphorylation is the measurement of mitochondrial oxygen consumption under different metabolic conditions.

Another way for ATP synthesis is through glycolysis. Glycolysis is a central ATP-producing pathway without the involvement of oxygen. It takes place in the cytoplasm of most cells. In the process of glycolysis, a glucose molecule with six carbon atoms is transformed into two pyruvate molecules, that each consists of three carbon atoms. In the end of glycolysis, the cell gains two molecules of ATP for each glucose molecule, that is catabolized into pyruvate. In addition, two molecules NADH are produced. These NADH molecules can further donate their electrons to the electron transport chain in aerobic organisms. The thereby formed NAD^+ molecules are again used for glycolysis (Alberts et al. 2015). To complete the glycolytic cycle in the absence of oxygen, pyruvate is transformed into lactic acid and NAD^+ by lactate dehydrogenase in the cytoplasm (Wu et al. 2007).

In some cancer cells, it is described that if they have mitochondrial metabolic defects through mutations in mitochondrial DNA, abnormal expression of enzymes of the energy metabolism or dysfunction of the electron transport chain, the cells shift their metabolism to glycolysis in order to maintain their energy supply. Thus, cancer cells are able to shift their metabolic pathways from mitochondrial oxidative phosphorylation to increased glycolysis to get enough ATP (Manzano et al. 2011). The Warburg effect of cancer cells is a specific characteristic of them. Therefore, they convert glucose into lactic acid even under normal oxygen tension. This process is also known as aerobic glycolysis (Wu et al. 2007).

The extracellular acidification rates (ECAR) can be measured during lactic acid formation in the glycolytic energy metabolism (Wu et al. 2007). Determination of ECAR through the proton liberation into the extracellular medium is thus one of many parameters for measuring the contribution of glycolytic activity in leishmanial energy production. Although ECAR are frequently used to report glycolytic rate, with the assumption that conversion of glucose to lactate and H^+ is the only significant source of acidification, another potential source of extracellular protons is the production of CO_2 during glucose oxidation.

Specifically, CO_2 generated in the citric acid cycle can be spontaneously hydrated to H_2CO_3 , which then dissociates to $\text{HCO}_3^- + \text{H}^+$. Without respiration-derived CO_2 correction to ECAR, the quantitative calculation of glycolytic rate is not possible (Mookerjee et al. 2015).

For the assessment of the contribution of lactate-associated glycolytic as well as respiration-derived mitochondrial pathways in leishmanial energy production under different metabolic conditions, various inhibitors of metabolism were applied (Figure 2).

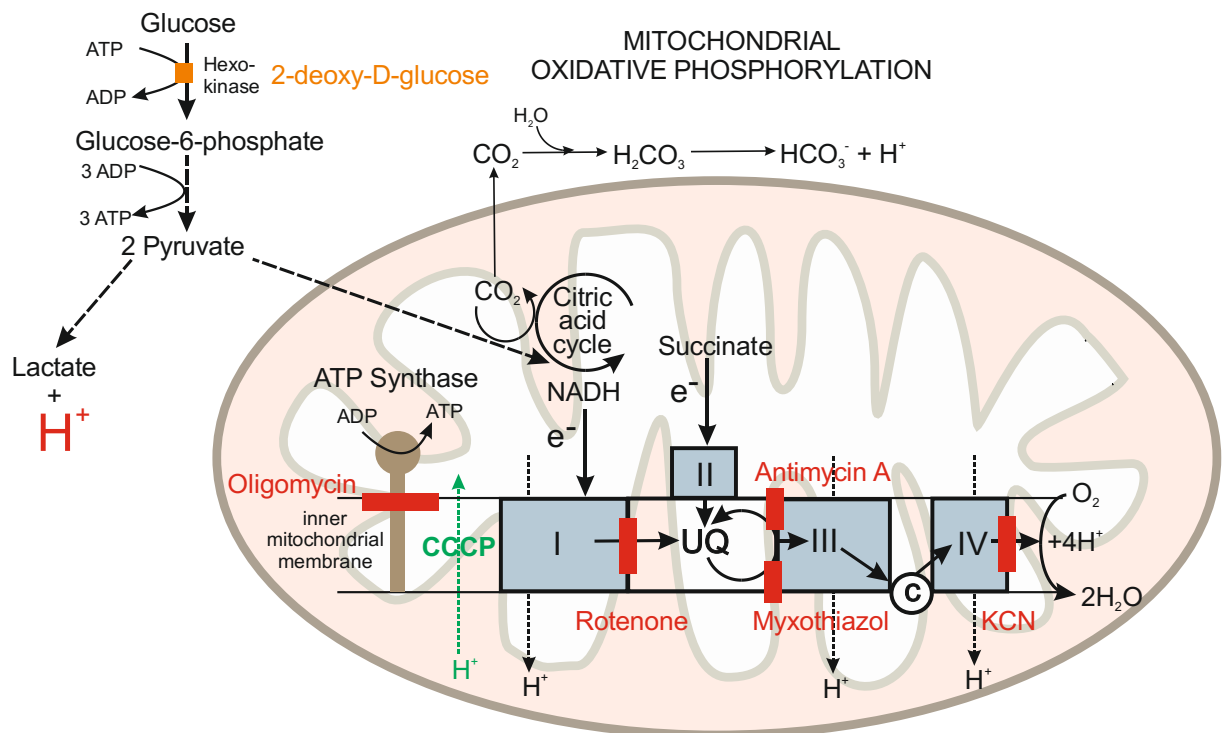


Figure 2: Glycolytic and oxidative mitochondrial pathways and their selective inhibitors

1.3 Inhibitors of metabolism

Rotenone is a mitochondrial complex I inhibitor. In *Leishmania donovani* promastigotes it was shown that this inhibitor has no effect on their oxygen consumption (Santhamma and Bhaduri 1995). The specific mitochondrial complex III inhibitor antimycin A is a natural toxin, that is produced by *Streptomyces* bacteria. Antimycin A inhibits the electron transfer from complex III to cytochrome c at the inner side of the inner mitochondrial membrane (Sakata-Kato and Wirth 2016). Myxothiazol, also a complex III inhibitor, stops the electron transport by the blockade of the reduction of cytochrome c at the outer side of the inner mitochondrial membrane (Meinhardt

and Crofts 1982). In *L. donovani* promastigotes, the complex IV inhibitor cyanide did not show a complete inhibition of the mitochondrial respiration (Santhamma and Bhaduri 1995).

Oligomycin inhibits the F_0F_1 -ATP synthase complex by blocking its proton channel in the inner mitochondrial membrane (Kathuria et al. 2014). This complex V inhibitor is commonly used for determination of the proportion of the oxygen consumption rate devoted to the mitochondrial ATP synthesis and the remaining proton leak in bioenergetic studies (Sakata-Kato and Wirth 2016).

Carbonyl cyanide m-chlorophenylhydrazone (CCCP) is an uncoupler of oxidative phosphorylation (Kathuria et al. 2014). Uncoupling agents dissipate the proton gradient across the inner membrane and are often used to quantify the respiratory reserve capacity by uncoupling the oxygen consumption at complex IV from the ATP synthesis at complex V (Sakata-Kato and Wirth 2016).

2-deoxy-D-glucose (2-DG) is an inhibitor of glycolysis. It restrains the reaction from glucose to glucose-6-phosphate in the glycolytic pathway (Sakata-Kato and Wirth 2016). Thus, it blocks the first step in glycolysis (Wu et al. 2007).

1.4 Aims of the study

The aim of this bachelor thesis was to investigate and compare the glycolytic and the mitochondrial function of *Leishmania tarentolae* promastigotes (LtP), particularly to assess:

1. the glycolytic activity of LtP by the measurement of the extracellular acidification rates (ECAR),
2. the oxidative mitochondrial function of LtP by the measurement of oxygen consumption rates,
3. the sensitivity of oxygen consumption rates and ECAR to different inhibitors of the mitochondrial respiratory chain (rotenone, antimycin A, myxothiazol), an ATP synthase inhibitor (oligomycin), an uncoupler of oxidative phosphorylation (carbonyl cyanide m-chlorophenylhydrazone) and an inhibitor of glycolysis (2-deoxy-D-glucose).

2 MATERIALS AND METHODS

2.1 Chemicals

The chemicals that were used for all experiments are listed in the following table.

Table 1: Used chemicals

Chemicals	Manufacturer	Purity
Antimycin A from <i>Streptomyces sp.</i>	Sigma	-
Boric acid	Merck	per analysis
Bovine serum albumin, fraction V	Fluka	> 96 %
Brain Heart Infusion (No. 53286 Brain Heart Broth)	Sigma-Aldrich	for microbiology
Carbonyl cyanide m-chlorophenylhydrazone (CCCP)	Sigma	-
Citric acid	Merck	for molecular biology
CuSO ₄ , pentahydrate	Merck	per analysis
D-(+)-glucose, monohydrate	Merck	for biochemical use
2-Deoxy-D-glucose	Sigma	≥ 99 %
Dimethyl sulfoxide (DMSO)	VWR (prolabo chemicals)	> 99.8 %
Hemin (porcine)	Sigma	-
HCl	Roth	per analysis
KCl	Merck	per analysis
KCN	Sigma	≥ 98 %

KH_2PO_4	Merck	per analysis
Myxothiazol	Sigma	-
NaCl	Merck	per analysis
Na_2HPO_4	Merck	per analysis
NaOH	Merck	per analysis
Oligomycin (mixture of A, B and C isomers)	Calbiochem	$\geq 90 \%$
Paraffin oil	Sigma-Aldrich	-
Penicillin (20,000 U/ml) / Streptomycin (20,000 $\mu\text{g/ml}$)	Lonza	-
Potassium iodide	Merck	per analysis
Potassium sodium tartrate, tetrahydrate	Merck	per analysis
Rotenone	Sigma	-
Sodium dithionite ($\text{Na}_2\text{S}_2\text{O}_4$)	Merck	per analysis
Trichloroacetic acid	Merck	per analysis

Ultrapure MQ-H₂O from a Milli Q[®] Advantage A10 water purification system (Merck Millipore, Darmstadt, Germany) was used for preparing aqueous solutions. Stock solutions of oligomycin (1.25 mM, 2.5 mM), CCCP (125 μM , 250 μM) antimycin A (2.5 μM , 5 μM , 10 μM , 25 μM , 40 μM), myxothiazol (0.625 mM, 1.25 mM, 2.5 mM, 5 mM, 10 mM, 20 mM), and rotenone (12.5 mM, 25 mM, 50 mM, 100 mM, 200 mM) were made in dimethyl sulfoxide (DMSO).

2.2 Cell culture of *Leishmania tarentolae* promastigote

Leishmania tarentolae promastigotes (LtP) of the LEXSY host strain P10 (Jena Bioscience GmbH, Jena, Germany; biosafety level 1) were used to carry out all experiments.

LtP were cultured in Brain Heart Infusion (BHI) medium at pH 7.4 and 26 °C in sterile 50 ml filter tubes (TubeSpin® Bioreactor 50, TTP, Trasadingen, Switzerland). The medium contained 37 g/l BHI, 5 mg/l hemin and, furthermore, 25,000 U/l penicillin and 25 mg/l streptomycin to prevent any bacterial contamination. The tubes with LtP suspensions were agitated on a shaker at 0.05 s⁻¹ inserted in an incubator (Ehret GmbH Life Science Solutions, Emmendingen, Germany). Passages of LtP were performed on Mondays, Wednesdays, and Fridays.

Ao. Univ. Prof. Dr. Lars Gille, Sara Todhe and Laura Machin cultivated and kindly provided *L. tarentolae* promastigotes for the experiments.

2.3 Determination of cell number

The LtP suspension was centrifuged in a Sorvall LYNX 6000 centrifuge (Thermo Fisher GmbH, Vienna, Austria) for 10 min at 25 °C and 1900 × g. The supernatant was then discarded. The pellet was resuspended in 10 ml of phosphate-buffered saline (PBS; 145.28 mM NaCl, 4.06 mM KCl, 160 μM Na₂HPO₄, 40 μM KH₂PO₄, adjusted to pH 7.4 with 0.1 M NaOH) and centrifuged again under the same conditions. The final pellet was resuspended in 5 ml PBS. Afterwards, the cell number of LtP was determined photometrically.

The optical density (OD) of a diluted LtP suspension was measured at a wavelength of 600 nm in 1.5 ml semi-micro cuvettes with a layer thickness of 1 cm (BRAND GmbH, Wertheim, Germany). The cell suspension was measured against a blank of PBS. The measured OD value was furthermore extrapolated to OD_{600 nm} value of the undiluted cell suspension.

The following formula for the determination of cell number in Yeast Extract Medium (Fritsche 2008) was used to calculate cell number in PBS:

$$\text{Cell number (10}^6 \text{ cells/ml)} = \text{OD}_{600 \text{ nm}} \times \text{dilution factor} \times 0.969 \times 124$$

0.969 conversion factor of g/l dry weight

124 1 g dry weight/l corresponds to 124 × 10⁶ cells/ml

The LtP suspension was diluted to a cell number of approximately 6 × 10⁸ LtP/ml PBS.

2.4 Determination of protein concentration

Duplicates of PBS-washed LtP suspensions (each 250 μ l) were frozen at -20 °C. Thawed samples were used to determine the protein concentration by the Biuret method. Therefore, 750 μ l MQ-H₂O and 200 μ l of 3 M trichloroacetic acid were added to the suspensions. The samples were incubated for 10 min at room temperature. Next, they were centrifuged for 10 min at 25 °C and 2500 \times g in a Micro Star 17R centrifuge (VWR, Vienna, Austria).

The supernatants were discarded and 1000 μ l Biuret solution (12.02 mM CuSO₄, 31.89 mM potassium sodium tartrate, 30.12 mM potassium iodide and 0.2 M NaOH) were added to each pellet. Afterwards the pellets were dissolved and incubated at room temperature for 10 min. The extinctions were measured with a U-1100 photometer (Hitachi Ltd., Tokyo, Japan) at 546 nm against a MQ-H₂O reference. Semi-micro cuvettes with a layer thickness of 1 cm were used. The blank values of Biuret solution were determined as the difference of extinctions in the absence and presence of KCN. The sample values were equally determined as the differences of extinctions measured at 546 nm before and after adding a spatula-tip of KCN to the samples. KCN was used to decolourise the blue copper-protein complexes in the samples and thus turbidity errors caused by interfering pigments or lipids can be eliminated (Bode et al. 1968). The blank value was subtracted from the sample value to calculate the difference of extinction (ΔE). The final protein concentration was determined using the following formulas.

$$\Delta E_{blank} = E_{blank-KCN} - E_{blank+KCN}$$

$$\Delta E_{sample} = E_{sample-KCN} - E_{sample+KCN}$$

$$\Delta E = \Delta E_{sample} - \Delta E_{blank}$$

$$c = \frac{\Delta E}{\varepsilon \times d} \times V_f$$

- c protein concentration in the sample [mg/ml]
- ε 0.21227 mg⁻¹ \times ml \times cm⁻¹ (extinction coefficient determined from a calibration curve using bovine serum albumin as a standard)
- d layer thickness of the cuvette (1 cm)
- V_f dilution factor (μ l total volume/ μ l sample volume)

2.5 Determination of oxygen consumption rates using OxoPlates®

2.5.1 Measurement principle of the OxoPlates® OP96U

OxoPlates® OP96U (PreSens, Regensburg, Germany) are sterile round bottom microplates in a 96-well format. They were applied for measuring oxygen consumption rates using the EnSpire® Multimode Plate Reader (Perkin Elmer Inc., Waltham, USA). According to the instruction manual of the manufacturer, each well has a sensor consisting of a thin polymer film at its base, which can be read out through the bottom of the plate. The sensor contains two different dyes, the indicator, and the reference dye. The fluorescence intensity of the indicator dye ($I_{indicator}$; excitation wavelength 540 nm, emission wavelength 650 nm) depends on the oxygen content in the well, while the fluorescence intensity of the reference dye ($I_{reference}$; excitation wavelength 540 nm, emission wavelength 590 nm) is independent of the oxygen content. The ratio I_R of these two fluorescence intensities is used for internal referencing of the sensor response in the applied fluorescence reader and calculation of the oxygen partial pressure, and subsequently oxygen concentration in each well.

$$I_R = \frac{I_{indicator}}{I_{reference}}$$

2.5.2 Calibration of OxoPlates® OP96U

The dry sensors of OxoPlates® needed to be equilibrated with samples for approximately 20 min. Before every experiment, a two-point calibration with oxygen-free PBS and air-saturated PBS was done. The two solutions were used to receive the calibration constants k_0 and k_{100} for calculation of oxygen concentrations. PBS with a few grains of sodium dithionite ($\text{Na}_2\text{S}_2\text{O}_4$) was used for determination of k_0 and air-saturated PBS was used for determination of k_{100} , respectively. For each calibration, 200 μl of dithionite-treated PBS was filled into six wells each. The same was done with air-saturated PBS. The samples were then closed by adding 70 μl of paraffin oil to each well to avoid interference of atmospheric oxygen into the results.

After measurement the fluorescence ratio I_R of each well was calculated with the formula above. Then, k_{100} was determined as the mean I_R of the six wells containing the air-saturated PBS and k_0 was determined as the mean I_R of the six wells containing the PBS with sodium dithionite.

Afterwards, the oxygen partial pressure pO_2 in % air saturation was calculated for each measuring point using the following formula.

$$pO_2 = 100 \times \frac{\left(\frac{k_0}{I_R} - 1\right)}{\left(\frac{k_0}{k_{100}} - 1\right)}$$

To transfer the oxygen unit from % air saturation to cO_2 [$\mu\text{mol/l}$] the pO_2 values were multiplied by factor f , according to the instruction manual of the manufacturer.

$$cO_2 [\mu\text{mol/l}] = pO_2 \times f$$

f 2.53 (multiplication factor, valid for $T = 26$ °C and atmospheric pressure = 1013 hPa)

2.5.3 Determination of oxygen consumption rates of *Leishmania tarentolae* promastigotes

After calibration of the OxoPlates® the measurements with LtP were performed. Therefore, 150 μl PBS was added into the remaining 84 wells, each. Furthermore, glucose (10 mM or 5 mM, final concentration) or MQ-H₂O, and the other reagents and inhibitors of interest in the desired final concentration were added. Each assay was performed in quadruplicates. The means were used for further statistical calculations.

The reaction was started by the addition of 50 μl of PBS-washed LtP into each well, to obtain a final cell number of around 1.5×10^8 LtP/ml or 1×10^8 LtP/ml, respectively. Afterwards the OxoPlate® was put on the Eppendorf Thermomixer R (Eppendorf AG, Hamburg, Germany) for 5 min at 25 °C and 800 rotations per min. Immediately thereafter, each well was covered by 70 μl paraffin oil. Then kinetic measurements for 40 min with 5 min intervals were done using the EnSpire® Multimode Plate Reader.

2.6 Determination of extracellular acidification rates using HydroPlates®

2.6.1 Measurement principle of the HydroPlates® HP96U

HydroPlates® HP96U (PreSens, Regensburg, Germany) are sterile round bottom microplates in a 96-well format. They were applied for measuring the extracellular acidification rates (ECAR) using the EnSpire® Multimode Plate Reader. According to the instruction manual of the manufacturer, each well has an optical sensor at its base, which can be read out through

the bottom of the plate. Every sensor contains two different dyes, one of which is the pH indicator, its fluorescence intensity ($I_{\text{indicator}}$; excitation wavelength 485 nm, emission wavelength 538 nm) is based on the pH of the sample. The other dye provides a reference, its fluorescence intensity ($I_{\text{reference}}$; excitation wavelength 485 nm, emission wavelength 620 nm) does not depend on the pH. The ratio I_R of these two fluorescence intensities is used for internal referencing of the sensor response in the applied fluorescence reader, and correlates to the pH.

$$I_R = \frac{I_{\text{indicator}}}{I_{\text{reference}}}$$

2.6.2 Calibration of HydroPlates® HP96U

The dry sensors of HydroPlates® needed to be equilibrated with samples for approximately 20 min. Before every experiment, a calibration was done, which determines the fluorescence ratios I_R of six different pH buffers. The pH 4 and pH 5 buffers contained 50 mM citric acid adjusted with 1 M NaOH to the desired pH values. The pH buffers for pH 6 and pH 7 contained 50 mM phosphate resulting from different ratios of Na_2HPO_4 and KH_2PO_4 . The pH buffers for pH 8 and pH 9 contained 50 mM boric acid adjusted with 1 M NaOH to the desired pH values. Each pH value was measured in duplicates. For each calibration point, 225 μl of 155 mM NaCl and 25 μl of the appropriate pH buffer were combined, giving a final concentration of 5 mM.

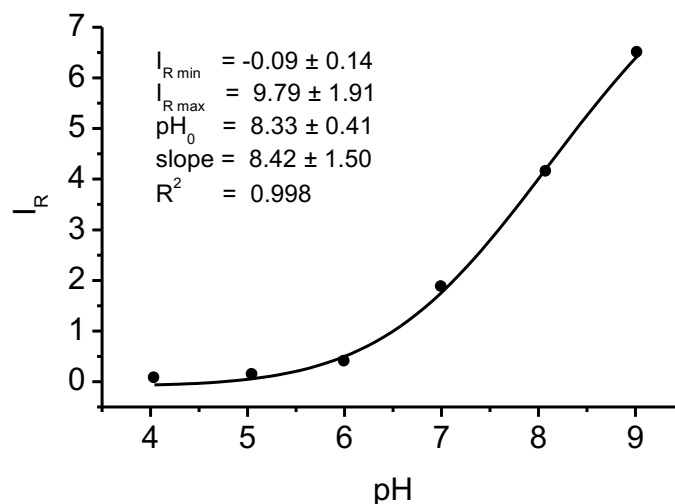


Figure 3: Representative calibration curve of HydroPlates® with respective pH buffers.

The calibration curve (Figure 3) was fitted via non-linear regression according to a four-parameter logistic model using the following formula:

$$I_R = I_{R \max} + \frac{I_{R \max} - I_{R \min}}{1 + (pH/pH_0)^{\text{slope}}}$$

After rearranging this formula, pH values were calculated accordingly.

$$pH = pH_0 \times \sqrt[\text{slope}]{\frac{I_{R \min} - I_{R \max}}{I_R - I_{R \max}} - 1}$$

2.6.3 Determination of extracellular acidification rates of *Leishmania tarentolae* promastigotes

After calibration of the HydroPlates[®] with pH 4 to 9 buffers, the measurements with LtP were performed. Therefore, 185 µl PBS was added into the remaining 84 wells, each. Furthermore, glucose (10 mM or 5 mM, final concentration) or MQ-H₂O, and the other reagents and inhibitors of interest in the desired final concentration were added. Each assay was performed in quadruplicates. The means were used for further statistical calculations.

The reaction was started by the addition of 65 µl of PBS-washed LtP into each well, to obtain a final cell number of around 1.5×10^8 LtP/ml or 1×10^8 LtP/ml, respectively. Afterwards the HydroPlate[®] was put on an Eppendorf Thermomixer R for 5 min at 25 °C and 800 rotations per min. Then kinetic measurements for 20 min with 5 min intervals were done using the EnSpire[®] Multimode Plate Reader.

2.7 Data analysis and statistics

Data were analysed by Microsoft[®] Excel 2016 and further processed by MicroCal Origin[®] 6.1 (OriginLab Corp., Northampton, MA, USA) for statistical analysis as well as for drawing figures. Data are shown as mean ± SEM (standard error of mean). All concentrations given in the figures or figure legends are final concentrations. Statistically significant differences between the respective experimental groups were identified using unpaired two-tailed Student's t-test.

3 RESULTS

3.1 Protein content of *Leishmania tarentolae* promastigotes

For the purpose of comparison with literature data, cell numbers and protein concentrations were photometrically determined. In 23 independent cell batches it was shown that 1×10^8 LtP corresponded to 0.212 ± 0.005 mg protein.

3.2 Determination of buffer factor

ECAR provide a qualitative measure of proton liberation into the extracellular medium. Since they are determined in mpH/min, they are dependent on the buffer capacity of the applied medium and the measurement system, i.e., buffers with higher buffer capacity will result in lower pH changes of the extracellular medium. For conversion of qualitative ECAR into quantitative proton efflux rates (PER), the knowledge of the buffer factor is necessary. The latter was determined by titration of the applied PBS containing 0.2 mM phosphate with increasing concentrations of HCl.

$$\text{PER} = \text{ECAR} \times \text{buffer factor} \times \text{sample volume}$$

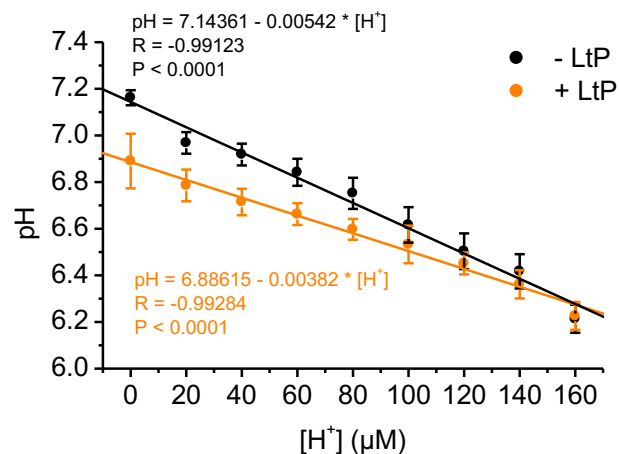


Figure 4: Linear regression between pH and $[H^+]$ in saline buffered with 0.2 mM phosphate (PBS) in the absence and presence of $1.588 \pm 0.048 \times 10^8/\text{ml}$ *Leishmania tarentolae* promastigotes (LtP). LtP were washed in glucose-free PBS. Data represent means \pm SEM of four independent cell batches.

The linear regression between pH and $[H^+]$ in PBS with and without PBS-washed LtP is illustrated in Figure 4. The samples with LtP started at a lower pH than those with no cells. The slope of the regression curve without LtP is a bit higher than the one with LtP (-0.00542 vs. -0.00382). From the slope of the curves a buffer factor of $185 \mu\text{M } H^+$ per 1 pH unit can be calculated for the applied PBS. In the presence of around 1.6×10^8 LtP/ml PBS the buffer factor was $262 \mu\text{M } H^+$ per 1 pH unit.

3.3 Oxygen consumption and extracellular acidification rates of *Leishmania tarentolae* promastigotes in the presence of mitochondrial inhibitors

3.3.1 Mitochondrial complex I inhibitor rotenone

The oxygen consumption rates (A, B) and ECAR (C, D) of LtP in the absence and presence of mitochondrial complex I inhibitor rotenone are depicted in Figure 5.

Basal oxygen consumption rates of LtP in PBS with 10 mM glucose normalized to 10^8 LtP were not significantly different when 1.57×10^8 LtP/ml instead of 1.05×10^8 LtP/ml were used in the assay ($2.72 \pm 0.28 \text{ nmol } O_2/\text{min}/10^8 \text{ LtP}$ vs. $2.85 \pm 0.42 \text{ nmol } O_2/\text{min}/10^8 \text{ LtP}$, $p > 0.05$; Figure 5, A and B). The addition of mitochondrial complex I inhibitor rotenone did not show any significant differences in both experimental setups, not even with increasing concentrations. A moderate but not significant decrease of oxygen consumption rates was observed in the presence of $50 \mu\text{M}$ rotenone. The only significant difference was observed in the absence of glucose, where the oxygen consumption rates of LtP decreased below the level of oxygen consumption rates with 10 mM glucose. The rates of LtP without glucose decreased to $1.09 \pm 0.14 \text{ nmol } O_2/\text{min}/10^8 \text{ LtP}$ for 1.57×10^8 LtP/ml and to $1.08 \pm 0.16 \text{ nmol } O_2/\text{min}/10^8 \text{ LtP}$ for 1.05×10^8 LtP/ml.

In the ECAR graphs, the same observations can be made as with the oxygen consumption rates. The basal ECAR of LtP in PBS with 10 mM glucose were $61.3 \pm 6.8 \text{ mpH}/\text{min}/10^8 \text{ LtP}$ for 1.63×10^8 LtP/ml and $58.5 \pm 7.5 \text{ mpH}/\text{min}/10^8 \text{ LtP}$ for 1.09×10^8 LtP/ml (Figure 5, C and D). By adding the mitochondrial complex I inhibitor rotenone, no significant differences were observed in each experimental setup, not even with increasing concentrations. The only significant decrease was found in LtP not supplemented with glucose. Here the ECAR decreased to $-2.2 \pm 1.9 \text{ mpH}/\text{min}/10^8 \text{ LtP}$ for 1.63×10^8 LtP/ml and $-4.8 \pm 1.6 \text{ mpH}/\text{min}/10^8 \text{ LtP}$ for 1.09×10^8 LtP/ml.

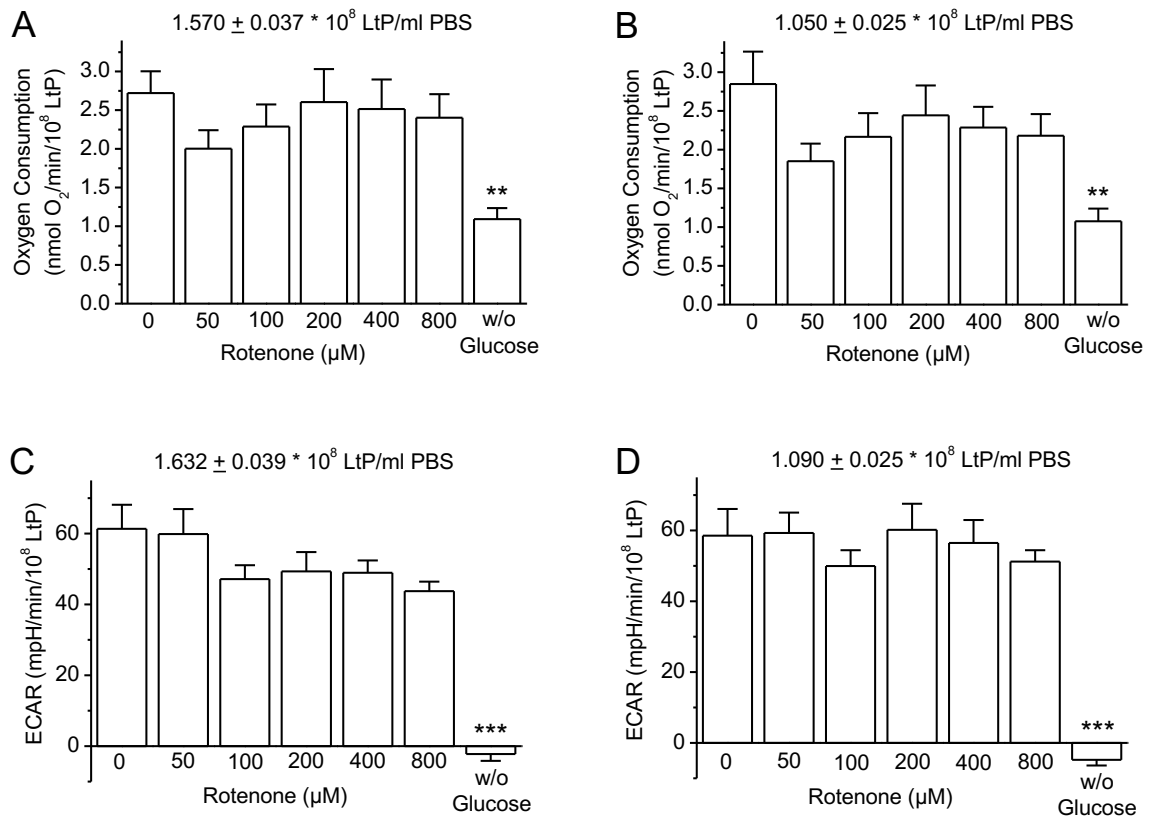


Figure 5: Oxygen consumption rates (A, B) and extracellular acidification rates (ECAR; C, D) of *Leishmania tarentolae* promastigotes (LtP) in the absence and presence of mitochondrial complex I inhibitor rotenone. LtP were washed in glucose-free phosphate-buffered saline (PBS) and analysed either in the presence of 10 mM glucose or in its absence (w/o glucose). Data represent means \pm SEM of four independent cell batches. **, *** indicate significant differences in comparison to control LtP (0 μM rotenone) at the level of $p < 0.01$ and 0.001 , respectively.

3.3.2 Mitochondrial complex III inhibitors antimycin A and myxothiazol

The oxygen consumption rates (A, B) and ECAR (C, D) of LtP in the absence and presence of mitochondrial complex III inhibitor antimycin A are shown in Figure 6.

Basal oxygen consumption rates of LtP in PBS with 10 mM glucose normalized to 10^8 LtP were not significantly different when 1.67×10^8 LtP/ml instead of 1.12×10^8 LtP/ml were used in the assay (1.96 ± 0.11 nmol O_2 /min/ 10^8 LtP vs. 1.84 ± 0.16 nmol O_2 /min/ 10^8 LtP, $p > 0.05$; Figure 6, A and B). A significant decrease of oxygen consumption can already be seen with the addition of 10 nM antimycin A in comparison to the control LtP not treated with antimycin A. With increasing concentrations of the inhibitor, a more significant decrease can be observed. The oxygen consumption with 20 nM antimycin A already decreased to 0.44 ± 0.10 nmol O_2 /min/ 10^8 LtP for 1.67×10^8 LtP/ml and 0.42 ± 0.05 nmol O_2 /min/ 10^8 LtP for 1.12×10^8 LtP/ml. The maximal effect on the oxygen consumption of LtP was observed in the presence of 80 nM antimycin A. A further increase of antimycin A concentration did not lead to an additional inhibition of oxygen consumption. Again, LtP not supplemented with glucose showed a significant decrease in oxygen consumption in relation to the control LtP supplemented with glucose.

The basal ECAR of LtP with 10 mM glucose were 42.0 ± 4.0 mpH/min/ 10^8 LtP for 1.65×10^8 LtP/ml and 38.4 ± 3.1 mpH/min/ 10^8 LtP for 1.10×10^8 LtP/ml (Figure 6, C and D). In contrast to the oxygen consumption rates, the addition of mitochondrial complex III inhibitor antimycin A showed no significant influence on ECAR until a concentration of 160 nM for 1.65×10^8 LtP/ml in comparison to control LtP (0 nM antimycin A). However, for 1.10×10^8 LtP/ml a significant decrease was already seen at a concentration of 80 nM antimycin A. In the absence of glucose ECAR were significantly decreased for both experimental setups, with an ECAR of -1.4 ± 1.9 mpH/min/ 10^8 LtP for 1.65×10^8 LtP/ml and -1.6 ± 2.4 mpH/min/ 10^8 LtP for 1.10×10^8 LtP/ml.

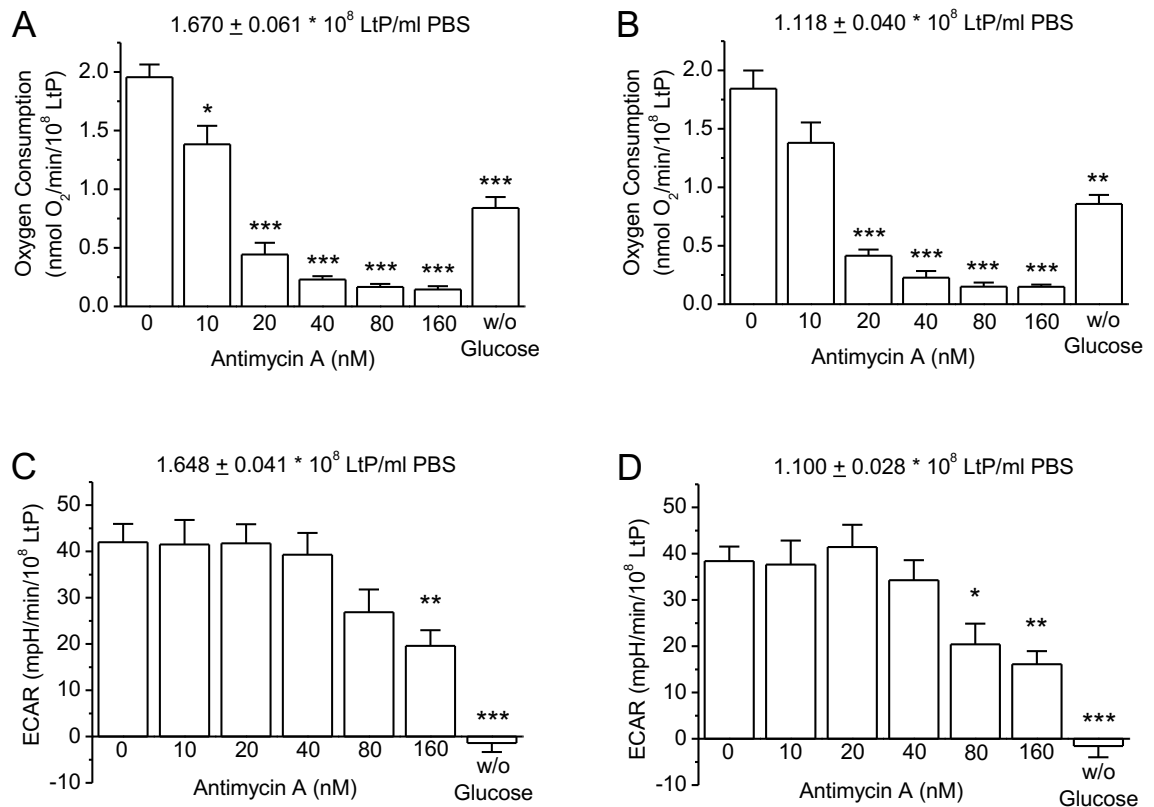


Figure 6: Oxygen consumption rates (A, B) and extracellular acidification rates (ECAR; C, D) of *Leishmania tarentolae* promastigotes (LtP) in the absence and presence of mitochondrial complex III inhibitor antimycin A. LtP were washed in glucose-free phosphate-buffered saline (PBS) and analysed either in the presence of 10 mM glucose or in its absence (w/o glucose). Data represent means \pm SEM of four independent cell batches. *, **, *** indicate significant differences in comparison to control LtP (0 nM antimycin A) at the level of $p < 0.05$, 0.01 and 0.001, respectively.

The oxygen consumption rates (A, B) and ECAR (C, D) of LtP in the absence and presence of mitochondrial complex III inhibitor myxothiazol are shown in Figure 7.

Basal oxygen consumption rates of LtP in PBS with 10 mM glucose were 1.87 ± 0.20 nmol O₂/min/10⁸ LtP for 1.72×10^8 LtP/ml and 1.63 ± 0.19 nmol O₂/min/10⁸ LtP for 1.15×10^8 LtP/ml (Figure 7, A and B). A significant decrease of oxygen consumption can already be seen in the presence of 10 μM myxothiazol in comparison to the control LtP with 0 μM myxothiazol. In the presence of 20 μM myxothiazol the effect on oxygen consumption rates was already at its maximum (0.53 ± 0.11 nmol O₂/min/10⁸ LtP for 1.72×10^8 LtP/ml; 0.39 ± 0.12 nmol O₂/min/10⁸ LtP for 1.15×10^8 LtP/ml) and could not be significantly increased any further by the addition of myxothiazol up to 80 μM. In the absence of glucose LtP also showed a significant decrease in oxygen consumption in relation to the glucose-supplemented control LtP.

The effect of myxothiazol on ECAR of LtP differed from that on oxygen consumption. The basal ECAR of LtP with 10 mM glucose and 0 μM myxothiazol were 37.0 ± 1.6 mpH/min/10⁸ LtP for 1.79×10^8 LtP/ml and 37.7 ± 0.8 mpH/min/10⁸ LtP for 1.20×10^8 LtP/ml (Figure 7, C and D). The addition of myxothiazol to 1.79×10^8 LtP/ml showed no significant difference in comparison to control LtP (0 μM myxothiazol). In contrast, for 1.20×10^8 LtP/ml a moderate, although significant decrease can be seen at a concentration of 40 μM myxothiazol. In the absence of glucose, ECAR showed significant decreases for both experimental setups, with an ECAR of -0.7 ± 0.4 mpH/min/10⁸ LtP for 1.79×10^8 LtP/ml and -0.8 ± 1.9 mpH/min/10⁸ LtP for 1.20×10^8 LtP/ml.

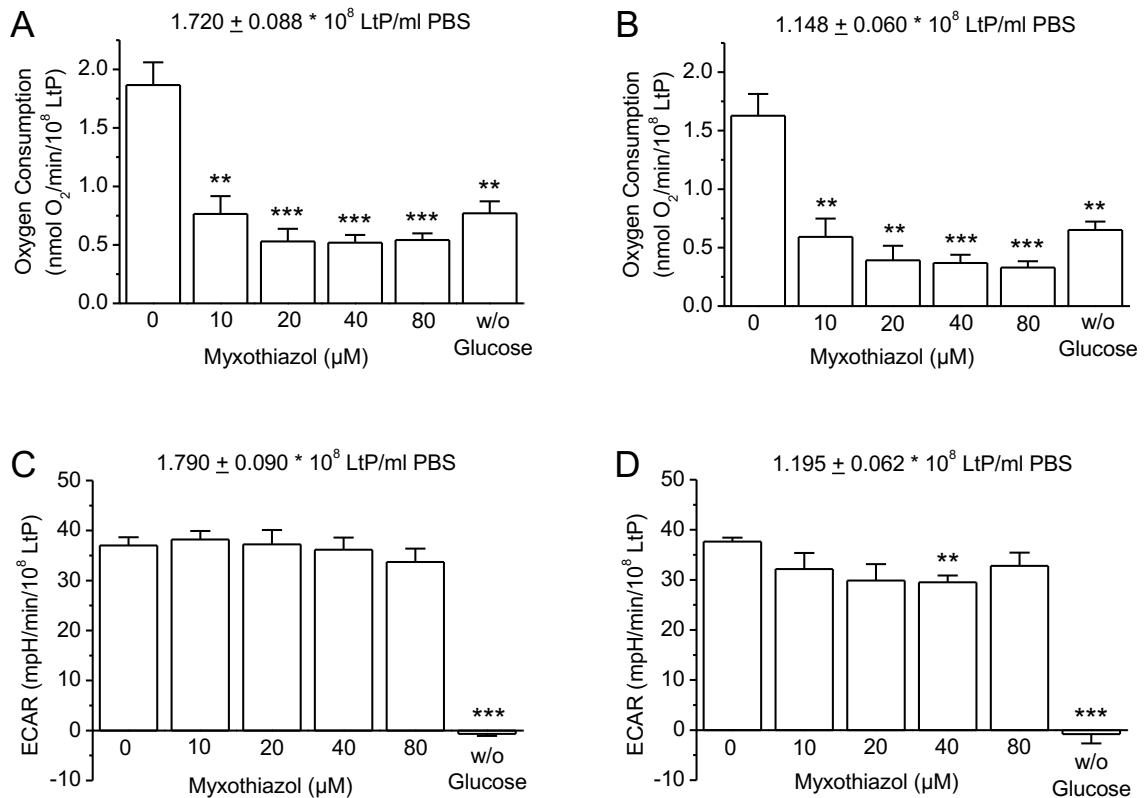


Figure 7: Oxygen consumption rates (A, B) and extracellular acidification rates (ECAR; C, D) of *Leishmania tarentolae* promastigotes (LtP) in the absence and presence of mitochondrial complex III inhibitor myxothiazol. LtP were washed in glucose-free phosphate-buffered saline (PBS) and analysed either in the presence of 10 mM glucose or in its absence (w/o glucose). Data represent means \pm SEM of four independent cell batches. **, *** indicate significant differences in comparison to control LtP (0 μM myxothiazol) at the level of $p < 0.01$ and 0.001 , respectively.

Due to an interference of cyanide, a mitochondrial complex IV inhibitor, with the fluorescence sensors of OxoPlates[®] (data not shown), this inhibitor cannot be used for a total blockade of the mitochondrial electron transport chain. Therefore, different combinations of complex III inhibitors myxothiazol and antimycin A were tested. The oxygen consumption rates (A) and ECAR (B) of LtP in the absence and presence of these mitochondrial complex III inhibitors are shown in Figure 8.

Basal oxygen consumption rates of LtP in PBS with 10 mM glucose and 0.8 % DMSO (vehicle) were 2.68 ± 0.20 nmol O₂/min/10⁸ LtP (Figure 8, A). With increasing myxothiazol concentrations up to 10 μM a significant decrease can be seen. Whereas 10 nM antimycin A moderately, although not significantly reduced the oxygen consumption. Nonetheless, 10 μM myxothiazol and 10 nM antimycin A in combination almost totally reduced the oxygen consumption to 0.08 ± 0.04 nmol O₂/min/10⁸ LtP (97 % inhibition).

The ECAR of LtP behaved in a different manner than the oxygen consumption rates. The basal ECAR of LtP with 10 mM glucose and 0.8 % DMSO were 55.9 ± 7.6 mpH/min/10⁸ LtP (Figure 8, B). The ECAR decreased a little by the addition of myxothiazol but showed no significant differences in comparison to control LtP (10 mM glucose and 0.8 % DMSO). 5 μM myxothiazol even slightly increased ECAR. Moreover, the combination of myxothiazol and antimycin A did not result in any significant changes in ECAR.

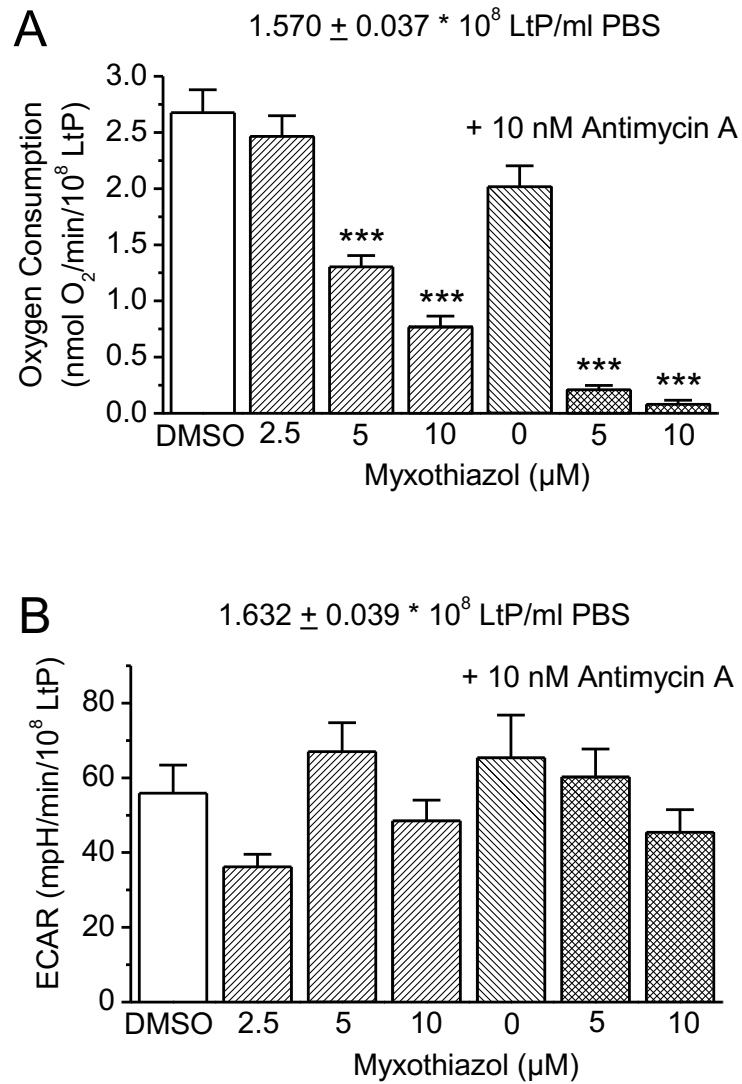


Figure 8: Oxygen consumption rates (A) and extracellular acidification rates (ECAR; B) of *Leishmania tarentolae* promastigotes (LtP) in the absence and presence of mitochondrial complex III inhibitors myxothiazol and antimycin A. LtP were analysed in phosphate-buffered saline (PBS) supplemented with 10 mM glucose. Data represent means \pm SEM of four independent cell batches. *** indicate significant differences in comparison to vehicle-treated LtP (DMSO, 0.8 %) at the level of $p < 0.001$.

3.4 Oxygen consumption and extracellular acidification rates of *Leishmania tarentolae* promastigotes in the presence of an ATP synthase inhibitor and an uncoupler

The oxygen consumption rates (A) and ECAR (B) of LtP in the absence and presence of the ATP synthase inhibitor oligomycin and the uncoupler CCCP are shown in Figure 9.

Basal oxygen consumption rates of vehicle-treated LtP (DMSO, 0.8 %) in PBS with 10 mM glucose were 1.95 ± 0.12 nmol O₂/min/10⁸ LtP (Figure 9, A). Oligomycin (5 μM and 10 μM) significantly decreased the oxygen consumption rates in comparison to the vehicle-treated LtP, while CCCP alone (0.5 μM and 1 μM) did not show any significant changes. However, CCCP significantly increased oligomycin (5 μM)-inhibited oxygen consumption rates (1.11 ± 0.01 nmol O₂/min/10⁸ LtP), both at 0.5 μM and 1 μM (2.22 ± 0.14 nmol O₂/min/10⁸ LtP and 2.01 ± 0.10 nmol O₂/min/10⁸ LtP; $p < 0.001$ vs. oligomycin-treated LtP).

ECAR of LtP showed a different picture in comparison to the results of the oxygen consumption rates. The basal ECAR of LtP with 10 mM glucose and 0.8 % DMSO were 38.2 ± 5.5 mpH/min/10⁸ LtP (Figure 9, B). The addition of the ATP synthase inhibitor oligomycin and the uncoupler CCCP, either alone or in combination, did not show any significant alterations in ECAR in comparison to the vehicle-treated LtP.

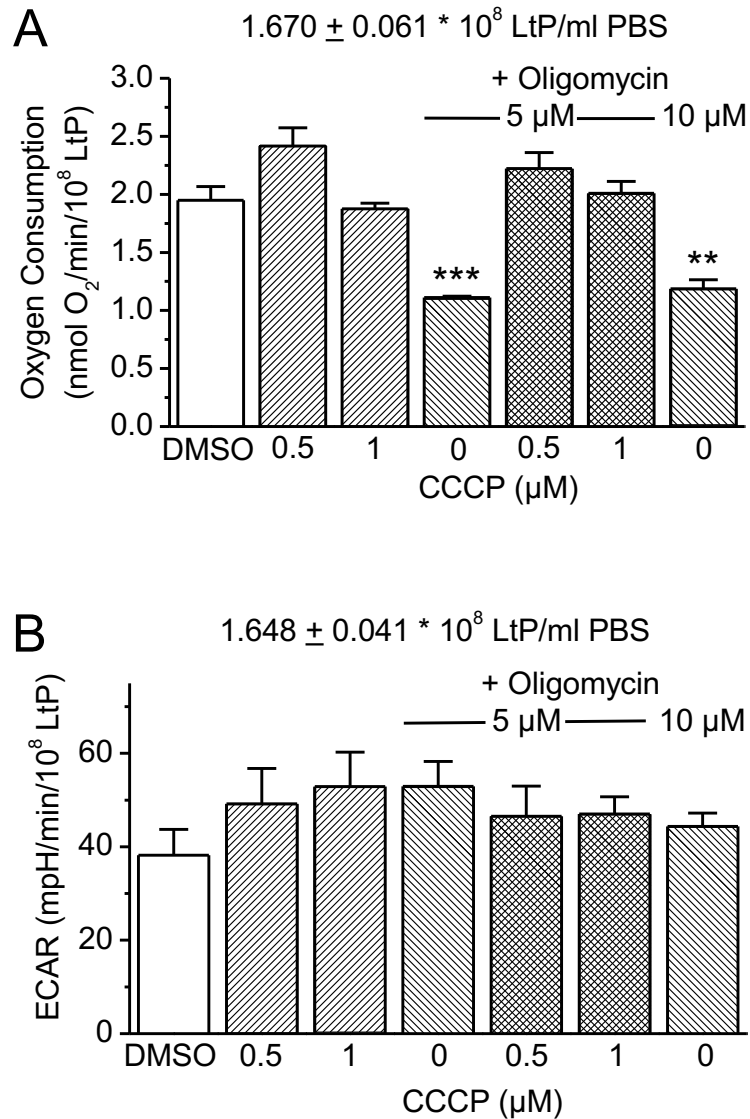


Figure 9: Oxygen consumption rates (A) and extracellular acidification rates (ECAR; B) of *Leishmania tarentolae* promastigotes (LtP) in the absence and presence of the ATP synthase inhibitor oligomycin and the uncoupler carbonyl cyanide m-chlorophenylhydrazone (CCCP). LtP were analysed in phosphate-buffered saline (PBS) supplemented with 10 mM glucose. Data represent means \pm SEM of four independent cell batches. **, *** indicate significant differences in comparison to vehicle-treated LtP (DMSO, 0.8 %) at the level of $p < 0.01$ and 0.001, respectively.

3.5 Mitochondrial bioenergetic vs. glycolytic activity of *Leishmania tarentolae* promastigotes

The oxygen consumption rates (A) and ECAR (B) of LtP in the absence and presence of the ATP synthase inhibitor oligomycin (5 μ M), the uncoupler CCCP (0.5 μ M) and complex III inhibitors myxothiazol (10 μ M) plus antimycin A (20 nM) are shown in Figure 10.

The basal oxygen consumption of untreated LtP in PBS with 5 mM glucose (control) was 2.48 ± 0.18 nmol O₂/min/10⁸ LtP (Figure 10, A). The oxygen consumption rates of LtP with oligomycin, CCCP and the two mitochondrial complex III inhibitors myxothiazol and antimycin A showed a significant decrease to 0.09 ± 0.02 nmol O₂/min/10⁸ LtP. Thus, only 3.6 % of oxygen consumption were of extra-mitochondrial origin. The addition of oligomycin alone resulted in a significant decrease of oxygen consumption to 1.48 ± 0.10 nmol O₂/min/10⁸ LtP. Taking the non-mitochondrial oxygen consumption into account, around 42 % of mitochondrial oxygen consumption were utilized for ATP production. The maximal oxygen consumption rates were observed in the presence of oligomycin in combination with CCCP (3.18 ± 0.31 nmol O₂/min/10⁸ LtP). These oxygen consumption rates revealed a spare capacity of mitochondrial oxygen consumption of around 29 % in comparison to basal mitochondrial oxygen consumption.

ECAR of LtP in the presence of oligomycin alone as well as in combination with CCCP did not show any significant changes in comparison to the control LtP. The basal ECAR of untreated LtP in PBS with 5 mM glucose (control) were 58.6 ± 7.0 mpH/min/10⁸ LtP (Figure 10, B). Surprisingly, the ECAR were significantly decreased with the combination of oligomycin, CCCP, myxothiazol and antimycin A.

In order to assess the contribution of glycolytic lactate production and mitochondrial CO₂ production in the ECAR, the proton efflux rates (PER) for both metabolic pathways were calculated. The total PER were derived from ECAR (Figure 10, B), as described in § 3.2, while PER associated with mitochondrial CO₂ production were determined from mitochondrial oxygen consumption rates (Figure 10, A). According to the following chemical reactions, one can assume that during oxidation of one molecule of glucose six H⁺ are liberated in parallel to the consumption of six O₂ molecules.



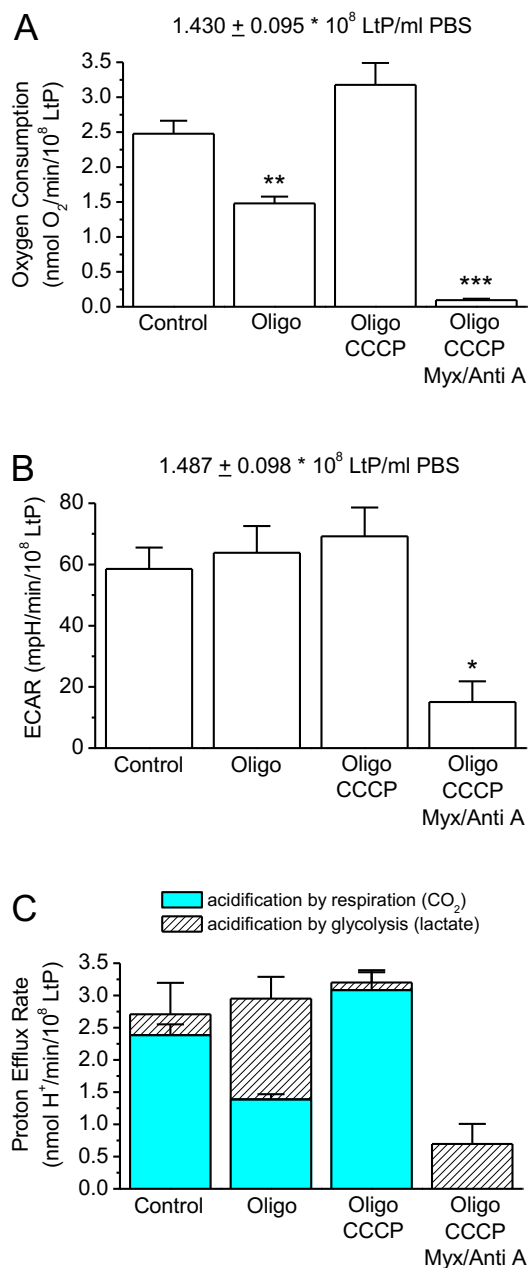


Figure 10: Oxygen consumption rates (A), extracellular acidification rates (ECAR; B), and proton efflux rates (C) of *Leishmania tarentolae* promastigotes (LtP) in the absence and presence of the ATP synthase inhibitor oligomycin (Oligo, 5 μ M), the uncoupler carbonyl cyanide m-chlorophenylhydrazone (CCCP, 0.5 μ M), and complex III inhibitors myxothiazol (Myx, 10 μ M) plus antimycin A (Anti A, 20 nM). LtP were analysed in phosphate-buffered saline (PBS) supplemented with 5 mM glucose. Data represent means \pm SEM of three independent cell batches. *, **, *** indicate significant differences in comparison to untreated LtP (Control) at the level of $p < 0.05$, 0.01 and 0.001, respectively.

Thus, for each O₂ molecule consumed one H⁺ is released into the extracellular medium. Furthermore, the glycolytic PER was calculated by subtracting the PER associated with mitochondrial CO₂ production from the total PER.

As can be seen in Figure 10 C, the respiratory CO₂ production substantially contributed to the total PER. In glucose-supplemented control LtP, only 11.8 % of PER were lactate-derived, while 88.2 % were CO₂-derived. In contrast, when mitochondrial ATP production was inhibited by oligomycin, the contribution of glycolysis in extracellular acidification increased to 52.9 %, while the contribution of mitochondrial CO₂ decreased to 47.1 % of total PER. After the addition of the uncoupler CCCP, the majority of total PER (96.2 %) was driven by CO₂ produced by mitochondrial respiration. The total inhibition of mitochondrial electron transport chain by antimycin A plus myxothiazol prevented oxygen consumption and, thus, mitochondria-associated extracellular acidification. The remaining 0.70 ± 0.31 nmol H⁺/min/10⁸ LtP were assumed to originate from glycolytic extracellular acidification.

3.6 Oxygen consumption and extracellular acidification rates of *Leishmania tarentolae* promastigotes in the presence of an inhibitor of glycolysis

The oxygen consumption rates (A) and ECAR (B) in the absence and presence of different concentrations of glucose and 2-deoxy-D-glucose (2-DG), an inhibitor of glycolysis, are shown in Figure 11.

Oxygen consumption rates of LtP supplemented with 1.25 - 10 mM glucose were not significantly inhibited in the presence of up to 10 mM 2-DG (Figure 11, A). Moreover, basal oxygen consumption rates of LtP in the absence of 2-DG did not significantly differ in the concentration range of 1.25 – 10 mM glucose. Nonetheless, oxygen consumption rates of LtP in the absence of glucose were significantly lower in comparison to oxygen consumption rates of LtP in the presence of 5 mM glucose (0.91 ± 0.06 nmol O₂/min/10⁸ LtP vs. 1.90 ± 0.02 nmol O₂/min/10⁸ LtP; $p < 0.001$) and were further reduced in the presence of 10 mM 2-DG.

ECAR of LtP supplemented with either 5 mM or 10 mM glucose were not significantly influenced by 2-DG concentrations up to 10 mM (Figure 11, B). However, in LtP supplemented with either 1.25 mM or 2.5 mM glucose, higher 2-DG concentrations significantly reduced ECAR. In the absence of glucose ECAR were significantly lower in comparison to ECAR of

LtP in the presence of 5 mM glucose (-5.1 ± 0.6 mpH/min/ 10^8 LtP vs. 38.6 ± 1.4 mpH/min/ 10^8 LtP; $p < 0.001$).

In an additional experiment it was found that ECAR of LtP supplemented with 5 mM glucose could be significantly reduced in the presence of 25 mM 2-DG (34.2 ± 4.6 mpH/min/ 10^8 LtP vs. 14.8 ± 1.8 mpH/min/ 10^8 LtP; $p < 0.05$).

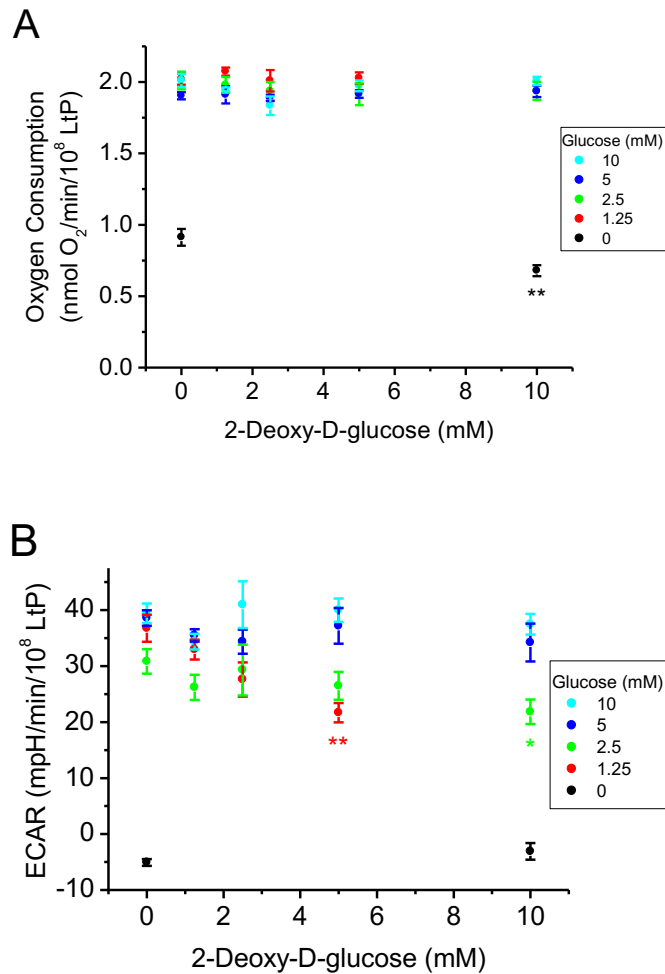


Figure 11: Oxygen consumption rates (A) and extracellular acidification rates (ECAR; B) of 1.42×10^8 /ml *Leishmania tarentolae* promastigotes (LtP). LtP were washed in glucose-free phosphate-buffered saline and analysed in the absence and presence of different concentrations of glucose and 2-deoxy-D-glucose (inhibitor of glycolysis). Data represent means \pm SEM of quadruplicates. *, ** indicate significant differences in comparison to the respective control LtP (0 mM 2-deoxy-D-glucose) at the level of $p < 0.05$ and 0.01, respectively.

3.7 Mitochondrial bioenergetic vs. glycolytic activity of *Leishmania tarentolae* promastigotes in the presence of different mitochondrial inhibitors and an inhibitor of glycolysis

The oxygen consumption rates (A and B) and ECAR (C and D) of LtP in the absence and presence of the ATP synthase inhibitor oligomycin (5 μ M), the mitochondrial complex III inhibitors myxothiazol (10 μ M) plus antimycin A (20 nM) and the glycolysis inhibitor 2-DG (25 mM) are shown in Figure 12.

Basal oxygen consumption of untreated LtP in PBS with 5 mM glucose were around 2.48 ± 0.18 nmol O₂/min/10⁸ LtP (Figure 12, A). In the absence of glucose oxygen consumption rates significantly decreased to 0.82 ± 0.11 nmol O₂/min/10⁸ LtP in relation to the LtP with glucose. The addition of oligomycin resulted in a significant decrease in oxygen consumption of glucose-supplemented LtP, while its combination with 2-DG did not result in a stronger inhibition (Figure 12, A). Oxygen consumption in the presence of myxothiazol and antimycin A significantly decreased to 0.03 ± 0.06 nmol O₂/min/10⁸ LtP (99 % inhibition). Combination of the complex III inhibitors with additional 2-DG did not result in a stronger inhibition (Figure 12, B).

The ECAR of LtP showed slightly different results than their oxygen consumption rates. The basal ECAR of untreated LtP with 5 mM glucose were 58.6 ± 7.0 mpH/min/10⁸ LtP (Figure 12, C) and decreased significantly to -0.4 ± 1.3 mpH/min/10⁸ LtP in the absence of glucose. The addition of oligomycin to glucose-supplemented LtP did not show significant changes in ECAR. However, the addition of 2-DG to oligomycin-inhibited LtP resulted in a moderate, although not significant decrease of ECAR (Figure 12, C). The ECAR of LtP with glucose, myxothiazol and antimycin A displayed a significant decrease to 11.9 ± 3.6 mpH/min/10⁸ LtP. With additional 2-DG the ECAR decreased even stronger to 0.1 ± 4.0 mpH/min/10⁸ LtP (Figure 12, D).

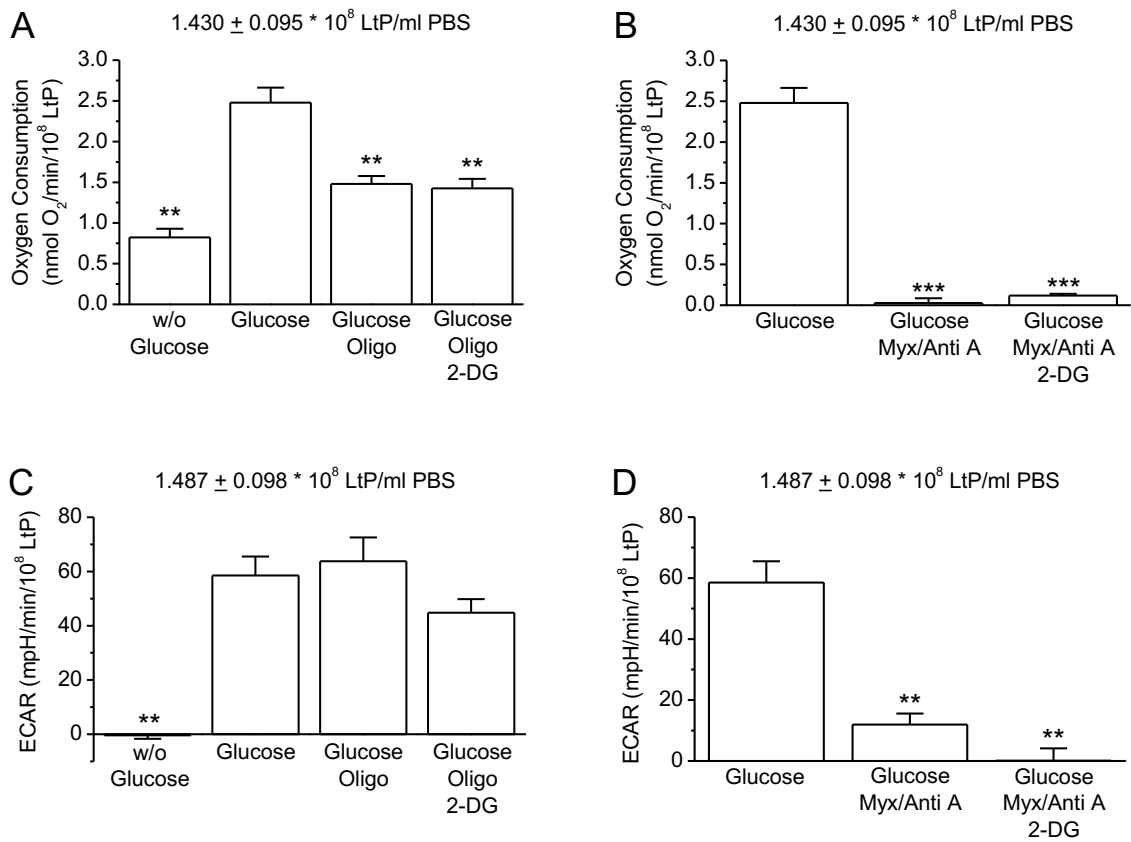


Figure 12: Oxygen consumption rates (A, B) and extracellular acidification rates (ECAR; C, D) of *Leishmania tarentolae* promastigotes (LtP). LtP were washed in glucose-free phosphate-buffered saline (PBS) and analysed in the absence and presence of the ATP synthase inhibitor oligomycin (Oligo, 5 μ M), complex III inhibitors myxothiazol (Myx, 10 μ M) plus antimycin A (Anti A, 20 nM), and the glycolysis inhibitor 2-deoxy-D-glucose (2-DG, 25 mM). Data represent means \pm SEM of three independent cell batches. **, *** indicate significant differences in comparison to untreated glucose-supplemented LtP (Glucose, 5 mM) at the level of $p < 0.01$ and 0.001, respectively.

4 DISCUSSION

The protozoan parasites of the genus *Leishmania* are the cause of different infectious diseases, for example leishmaniasis (Fidalgo and Gille 2011). Since leishmaniasis poses a danger to over 350 million people worldwide, the understanding of the diversity of *Leishmania* spp. and the development of treatment options seems to be more and more important (Kaye and Scott 2011). For therapeutic strategies the single mitochondrion of *Leishmania* is a possible target and, thus, an interesting subject of research (Fidalgo and Gille 2011). The different physiological and metabolic adaptations to extremely diverse environments of the two life stages of *Leishmania*, the extracellular promastigotes and the intracellular amastigotes, should be considered as well (Rosenzweig et al. 2008). Thus, the contribution of glycolytic and oxidative mitochondrial pathways to leishmanial energy production are of interest. Therefore, this study focused on the investigation and comparison of the glycolytic and the mitochondrial function of *Leishmania tarentolae* promastigotes (LtP).

The complex I inhibitor rotenone (up to 800 μM) was shown to have no influence on the mitochondrial O_2 consumption nor on the extracellular acidification rates (ECAR) of LtP. Santhamma and Bhaduri observed that the respiration of *Leishmania donovani* promastigotes is insensitive to this inhibitor up to a concentration of 320 μM (Santhamma and Bhaduri 1995). Thus, our results align with the findings by Santhamma and Bhaduri, meaning that rotenone does not seem to have an effect on leishmanial metabolic functions (Santhamma and Bhaduri 1955). In contrast, it was shown that human tumor cells are sensitive to this complex I inhibitor already at a concentration of 1 μM . Therefore, it is possible that the leishmanial complex I differs from the mammalian one (Wu et al. 2007).

The oxygen consumption rates of LtP were significantly decreased in the presence of the complex III inhibitor antimycin A up to a concentration of 160 nM. Leishmanial ECAR were not influenced by the addition of the inhibitor representatively, only at high concentrations a decrease in ECAR was shown. The findings regarding oxygen consumption correspond to the results of Santhamma and Bhaduri in *L. donovani*, where the reduced ubiquinone:cytochrome c reductase inhibitor antimycin A was also effective already at very low concentrations (Santhamma and Bhaduri 1995). Even in other protozoan parasites, like *Plasmodium falciparum*, which are the cause of malaria in humans, it was shown that antimycin A decreased oxygen consumption rates, but also had no significant effect on ECAR (Sakata-Kato and Wirth 2017).

Myxothiazol, another mitochondrial complex III inhibitor, showed very similar results to the oxygen consumption rates and ECAR of LtP with antimycin A. Nonetheless, the combination of 10 nM antimycin A and 10 μ M myxothiazol showed a higher inhibition of the oxygen consumption in LtP than each inhibitor alone (97 % vs. 25 % by antimycin A and 71 % by myxothiazol), which suggests an additive effect of these two complex III inhibitors.

The ATP synthase inhibitor oligomycin can be used to assess the proportion of oxygen consumption that is utilized for ATP production as well as that resulting from proton leak (Hill et al. 2012). Oligomycin (5 μ M) significantly inhibited the glucose-dependent O₂ consumption of LtP by 42 %, when taking the non-mitochondrial oxygen consumption into account. However, ECAR were only moderately enhanced, thus reflecting a rather small glycolytic reserve capacity of LtP. In contrast, in glucose-supplemented rat skeletal muscle cells, it was shown, that after treatment with oligomycin (800 nM) the cells were able to upregulate glycolysis to gain enough ATP despite the blockade of mitochondrial ATP synthesis, while oxygen consumption was decreased by approximately 60 % (Dott et al. 2014).

In previous studies it was shown that carbonyl cyanide m-chlorophenylhydrazone (CCCP) is a functional uncoupler of oxidative phosphorylation in leishmanial mitochondria (Monzote et al. 2018). Through the addition of the uncoupler the inner mitochondrial membrane gets permeable to protons and thus the control over the electron transfer is no longer reliant on the proton gradient. Hence, the oxygen consumption of the cells increased (Hill et al. 2012). The combination of oligomycin and the uncoupler CCCP resulted in maximal oxygen consumption rates of LtP. These oxygen consumption rates revealed a spare capacity of mitochondrial oxygen consumption of around 29 % in comparison to basal mitochondrial oxygen consumption. In the study of Dott et al. the uncoupler carbonyl cyanide 4-(trifluoromethoxy)phenylhydrazone (800 nM) increased the oxygen consumption rate by around 50 % in comparison to the basal oxygen consumption rate of the skeletal muscle cells (Dott et al. 2014).

For the inhibition of the electron transport chain of LtP, we used a combination of the two complex III inhibitors antimycin A (20 nM) and myxothiazol (10 μ M). The significant decrease by approximately 96 % showed that 3.6 % of oxygen consumption were of extra-mitochondrial origin. In comparison, in rat skeletal muscle cells antimycin A (200 nM) decreased the O₂ consumption by over 87 % compared to basal oxygen consumption rates. Thus, around 13 % were attributed to non-mitochondrial oxygen-consuming processes (Dott et al. 2014).

The addition of an inhibitor of glycolysis, namely 2-deoxy-D-glucose (2-DG), resulted in a sharp decrease in the ECAR in *Plasmodium falciparum*, which seems to be an indication for the glycolytic activity in these parasites. For the oxygen consumption rates of these parasites only a transient increase was described (Sakata-Kato and Wirth 2017). Our studies showed that 2-DG (25 mM) decreased ECAR of glucose-supplemented (5 mM) control LtP, but only by 57 %. Furthermore, the addition of 2-DG to oligomycin-inhibited LtP resulted in a 30 % decrease of ECAR. In contrast, the leishmanial O₂ consumption was not influenced by 2-DG. The addition of 2-DG to oligomycin-inhibited LtP resulted in a 4 % decrease of O₂ consumption rates only. One possible reason could be that the final concentration of 2-DG was not high enough in our assay.

It is known that the extracellular acidification rates can result not only from the glycolytic lactate-dependent acidification rates, but also from mitochondrial respiratory CO₂-dependent acidification rates. Therefore, determination of glycolytic rate using extracellular acidification requires differentiation between respiratory and glycolytic acid production (Mookerjee et al. 2015). In the present study, it was found that in glucose-supplemented control LtP the mitochondrial CO₂ production substantially contributed to the total proton efflux rates. In contrast, in the presence of the ATP synthase inhibitor oligomycin it was observed that the contribution of glycolysis in extracellular acidification increased to 52.9 %, while the contribution of mitochondrial CO₂ decreased to 47.1 % of total proton efflux rates.

In conclusion, the contribution of glycolytic and oxidative mitochondrial pathways to leishmanial energy production can be assessed by determination of leishmanial oxygen consumption rates in parallel with the extracellular acidification rates in the same cell batches under different metabolic conditions if the proportion of mitochondrially derived CO₂ in extracellular acidification rates is taken into consideration.

5 SUMMARY

Parasitic protozoa of the genus *Leishmania* cause the disease leishmaniasis. *Leishmania* live as extracellular promastigotes in the sandfly vector and as intracellular amastigotes in macrophages of the host. These two forms survive under different conditions, such as pH values, temperatures, different availability of energy sources (glucose, amino acids, fatty acids). As *Leishmania* possess a glycosome and a single mitochondrion, they are hypothesized to gain energy via glycolytic lactate-derived as well as oxidative mitochondrial pathways. Depending on the metabolic situation the proportion of these pathways is supposed to change.

In this bachelor thesis, non-human-pathogenic *Leishmania tarentolae* promastigotes (LtP) were studied. Their oxidative mitochondrial function was analysed using OxoPlates® with integrated fluorescence O₂ sensors and a fluorescence plate reader. Extracellular acidification rates (ECAR) were determined using HydroPlates® with integrated fluorescence pH indicators. The aim of this study was to investigate the contribution of glycolysis in leishmanial energy production by measuring ECAR.

Results have shown that the complex I inhibitor rotenone (up to 800 µM) has no influence on mitochondrial O₂ consumption and ECAR of *Leishmania*, while complex III inhibitors antimycin A (≥ 10 nM) and myxothiazol (≥ 10 µM) significantly decreased O₂ consumption. Surprisingly, ECAR were not stimulated in their presence, but even decreased. While in the absence of glucose O₂ consumption of LtP decreased only by around 60 %, their ECAR were completely inhibited. Moreover, 2-deoxy-D-glucose (inhibitor of glycolysis; 25 mM) did not influence O₂ consumption of glucose-supplemented (5 mM) LtP, while decreasing leishmanial ECAR by 57 %. The ATP synthase inhibitor oligomycin (5 µM) inhibited glucose-dependent O₂ consumption by 42 %, while ECAR were only moderately enhanced. However, considering the contribution of mitochondrial CO₂-derived ECAR in total ECAR, we could demonstrate that the proportion of glycolytic to oxidative mitochondrial pathways is shifted to a higher glycolytic state in comparison to control LtP (52.9 % vs. 11.8 %).

6 ZUSAMMENFASSUNG

Parasitische Protozoen der Gattung *Leishmania* verursachen die Krankheit Leishmaniose. Leishmanien leben als extrazelluläre Promastigoten in Sandfliegen als Vektor und als intrazelluläre Amastigoten in den Makrophagen des Wirts. Diese zwei Lebensformen überleben bei unterschiedlichen Bedingungen, wie pH, Temperatur, verschiedenen Energiequellen (Glukose, Aminosäuren, Fettsäuren). Da Leishmanien ein Glykosom und ein einzelnes Mitochondrium besitzen, wird angenommen, dass sie ihre Energie sowohl durch glykolytische Laktat-abhängige als auch durch oxidative mitochondriale Stoffwechselwege gewinnen. In Abhängigkeit von der Stoffwechselsituation kann sich das Verhältnis dieser Stoffwechselwege ändern.

In dieser Bachelorarbeit wurden für den Menschen nicht pathogene *Leishmania tarentolae* Promastigoten (LtP) untersucht. Deren oxidative mitochondriale Funktion wurde mittels OxoPlates[®] mit integrierten fluoreszierenden O₂-Sensoren und einem Fluoreszenz-Plattenlesegerät analysiert. Die extrazellulären Versauerungsraten (ECAR) wurden mittels HydroPlates[®] mit integrierten fluoreszierenden pH-Indikatoren bestimmt. Das Ziel dieser Untersuchungen war es, die Beteiligung der Glykolyse an der Energieproduktion von Leishmanien mittels ECAR zu untersuchen.

Die Ergebnisse haben gezeigt, dass der Komplex I Inhibitor Rotenon (bis zu 800 µM) keinen Einfluss auf den mitochondrialen O₂-Verbrauch und die ECAR von Leishmanien hat, während die Komplex III Inhibitoren Antimycin A (≥ 10 nM) und Myxothiazol (≥ 10 µM) den O₂-Verbrauch signifikant reduziert haben. Überraschenderweise wurden die ECAR in deren Anwesenheit nicht stimuliert, sondern nahmen sogar ab. Während der O₂-Verbrauch der LtP in Abwesenheit von Glukose nur um rund 60 % gesenkt wurde, wurden die ECAR vollständig inhibiert. Außerdem zeigte 2-Desoxy-D-glukose (Inhibitor der Glykolyse; 25 mM) keinen Einfluss auf den O₂-Verbrauch von Glukose-angereicherten (5 mM) LtP, während die ECAR von Leishmanien um 57 % gesenkt wurden. Der ATP Synthase Inhibitor Oligomycin (5 µM) hemmte den Glukose-abhängigen O₂-Verbrauch um 42 %, während die ECAR nur moderat erhöht wurden. Allerdings konnte gezeigt werden, dass sich das Verhältnis des glykolytischen zum oxidativen mitochondrialen Stoffwechselweg in Richtung eines höheren glykolytischen Status im Vergleich zu Kontroll-LtP verschiebt (52,9 % vs. 11,8 %), wenn man den Anteil der mitochondrialen CO₂-abhängigen ECAR an der totalen ECAR berücksichtigt.

7 LIST OF ABBREVIATIONS

2-DG	2-deoxy-D-glucose
ADP	adenosine diphosphate
Anti A	antimycin A
ATP	adenosine triphosphate
BHI	Brain Heart Infusion
CCCP	carbonyl cyanide m-chlorophenylhydrazone
DMSO	dimethyl sulfoxide
ECAR	extracellular acidification rates
LtP	<i>Leishmania tarentolae</i> promastigotes
Myx	myxothiazol
NADH/NAD ⁺	nicotinamide adenine dinucleotide
OD	optical density
Oligo	oligomycin
PBS	phosphate-buffered saline
PER	Proton efflux rates
SEM	standard error of mean

8 LIST OF FIGURES

Figure 1: Life cycle of the genus <i>Leishmania</i>	2
Figure 2: Glycolytic and oxidative mitochondrial pathways and their selective inhibitors	5
Figure 3: Representative calibration curve of HydroPlates® with respective pH buffers.	13
Figure 4: Linear regression between pH and [H ⁺] in saline buffered with 0.2 mM phosphate (PBS) in the absence and presence of $1.588 \pm 0.048 \times 10^8$ /ml <i>Leishmania tarentolae</i> promastigotes (LtP). LtP were washed in glucose-free PBS. Data represent means \pm SEM of four independent cell batches.....	15
Figure 5: Oxygen consumption rates (A, B) and extracellular acidification rates (ECAR; C, D) of <i>Leishmania tarentolae</i> promastigotes (LtP) in the absence and presence of mitochondrial complex I inhibitor rotenone. LtP were washed in glucose-free phosphate-buffered saline (PBS) and analysed either in the presence of 10 mM glucose or in its absence (w/o glucose). Data represent means \pm SEM of four independent cell batches. **, *** indicate significant differences in comparison to control LtP (0 μ M rotenone) at the level of $p < 0.01$ and 0.001 , respectively.....	17
Figure 6: Oxygen consumption rates (A, B) and extracellular acidification rates (ECAR; C, D) of <i>Leishmania tarentolae</i> promastigotes (LtP) in the absence and presence of mitochondrial complex III inhibitor antimycin A. LtP were washed in glucose-free phosphate-buffered saline (PBS) and analysed either in the presence of 10 mM glucose or in its absence (w/o glucose). Data represent means \pm SEM of four independent cell batches. *, **, *** indicate significant differences in comparison to control LtP (0 nM antimycin A) at the level of $p < 0.05$, 0.01 and 0.001 , respectively.....	19
Figure 7: Oxygen consumption rates (A, B) and extracellular acidification rates (ECAR; C, D) of <i>Leishmania tarentolae</i> promastigotes (LtP) in the absence and presence of mitochondrial complex III inhibitor myxothiazol. LtP were washed in glucose-free phosphate-buffered saline (PBS) and analysed either in the presence of 10 mM glucose or in its absence (w/o glucose). Data represent means \pm SEM of four independent cell batches. **, *** indicate significant differences in comparison to control LtP (0 μ M myxothiazol) at the level of $p < 0.01$ and 0.001 , respectively.....	21
Figure 8: Oxygen consumption rates (A) and extracellular acidification rates (ECAR; B) of <i>Leishmania tarentolae</i> promastigotes (LtP) in the absence and presence of mitochondrial	

complex III inhibitors myxothiazol and antimycin A. LtP were analysed in phosphate-buffered saline (PBS) supplemented with 10 mM glucose. Data represent means \pm SEM of four independent cell batches. *** indicate significant differences in comparison to vehicle-treated LtP (DMSO, 0.8 %) at the level of $p < 0.001$23

Figure 9: Oxygen consumption rates (A) and extracellular acidification rates (ECAR; B) of *Leishmania tarentolae* promastigotes (LtP) in the absence and presence of the ATP synthase inhibitor oligomycin and the uncoupler carbonyl cyanide m-chlorophenylhydrazone (CCCP). LtP were analysed in phosphate-buffered saline (PBS) supplemented with 10 mM glucose. Data represent means \pm SEM of four independent cell batches. **, *** indicate significant differences in comparison to vehicle-treated LtP (DMSO, 0.8 %) at the level of $p < 0.01$ and 0.001 , respectively.....25

Figure 10: Oxygen consumption rates (A), extracellular acidification rates (ECAR; B), and proton efflux rates (C) of *Leishmania tarentolae* promastigotes (LtP) in the absence and presence of the ATP synthase inhibitor oligomycin (Oligo, 5 μ M), the uncoupler carbonyl cyanide m-chlorophenylhydrazone (CCCP, 0.5 μ M), and complex III inhibitors myxothiazol (Myx, 10 μ M) plus antimycin A (Anti A, 20 nM). LtP were analysed in phosphate-buffered saline (PBS) supplemented with 5 mM glucose. Data represent means \pm SEM of three independent cell batches. *, **, *** indicate significant differences in comparison to untreated LtP (Control) at the level of $p < 0.05$, 0.01 and 0.001 , respectively.27

Figure 11: Oxygen consumption rates (A) and extracellular acidification rates (ECAR; B) of 1.42×10^8 /ml *Leishmania tarentolae* promastigotes (LtP). LtP were washed in glucose-free phosphate-buffered saline and analysed in the absence and presence of different concentrations of glucose and 2-deoxy-D-glucose (inhibitor of glycolysis). Data represent means \pm SEM of quadruplicates. *, ** indicate significant differences in comparison to the respective control LtP (0 mM 2-deoxy-D-glucose) at the level of $p < 0.05$ and 0.01 , respectively.29

Figure 12: Oxygen consumption rates (A, B) and extracellular acidification rates (ECAR; C, D) of *Leishmania tarentolae* promastigotes (LtP). LtP were washed in glucose-free phosphate-buffered saline (PBS) and analysed in the absence and presence of the ATP synthase inhibitor oligomycin (Oligo, 5 μ M), complex III inhibitors myxothiazol (Myx, 10 μ M) plus antimycin A (Anti A, 20 nM), and the glycolysis inhibitor 2-deoxy-D-glucose

(2-DG, 25 mM). Data represent means \pm SEM of three independent cell batches. **, *** indicate significant differences in comparison to untreated glucose-supplemented LtP (Glucose, 5 mM) at the level of $p < 0.01$ and 0.001 , respectively. 31

9 REFERENCES

- Alberts B, Johnson A, Lewis J, Morgan D, Raff M, Roberts K, Walter P. 2015. *Molecular Biology of The Cell*. Sixth edition. New York: Garland Science, 74-75.
- Bode C, Goebell H, Stähler E. 1968. Zur Eliminierung von Trübungsfehlern bei der Eiweißbestimmung mit der Biuretmethod. *Zeitschrift für klinische Chemie und klinische Biochemie*, 6(5):418–422.
- Burchmore RJS, Hart DT. 1995. Glucose transport in amastigotes and promastigotes of *Leishmania mexicana mexicana*. *Molecular and Biochemical Parasitology*, 74(1):77-86.
- Chakraborty B, Biswas S, Mondal S, Bera T. 2010. Stage specific developmental changes in the mitochondrial and surface membrane associated redox systems of *Leishmania donovani* promastigote and amastigote. *Biochemistry (Moscow)*, 75(4):494–518.
- Dott W, Mistry P, Wright J, Cain K, Herbert KE. 2014. Modulation of mitochondrial bioenergetics in a skeletal muscle cell line model of mitochondrial toxicity. *Redox Biology*, 2:224-233.
- Fidalgo LM, Gille L. 2011. Mitochondria and *trypanosomatids*: Targets and drugs. *Pharmaceutical Research*, 28(11):2758–2770.
- Fritsche C. 2008. Untersuchungen zur optimalen Kultivierung von *Leishmania tarentolae* [Dissertation]. Halle-Wittenberg: Martin-Luther-Universität.
- Hill BG, Benavides GA, Lancaster JR Jr, Ballinger S, Dell'Italia L, Jianhua Z, Darley-Usmar VM. 2012. Integration of cellular bioenergetics with mitochondrial quality control and autophagy. *Biological Chemistry*, 393(12):1485-1512.
- Kathuria M, Bhattacharjee A, Sashidhara KV, Singh SP, Mitra K. 2014. Induction of mitochondrial dysfunction and oxidative stress in *Leishmania donovani* by orally active clerodane diterpene. *Antimicrobial Agents and Chemotherapy*, 58(10):5916-5928.
- Kaye P, Scott P. 2011. Leishmaniasis: Complexity at the host-pathogen interface. *Nature Reviews Microbiology*, 9(8):604–615.
- Klatt S, Simpson L, Maslov DA, Konthur Z. 2019. *Leishmania tarentolae*: Taxonomic classification and its applicationx as a promising biotechnological expression host. *PLoS Neglected Tropical Diseases*, 13(7):e0007424.

- Manzano JI, Carvalho L, Pérez-Victoria JM, Castanys S, Gamarro F. 2011. Increased glycolytic ATP synthesis is associated with tafenoquine resistance in *Leishmania major*. *Antimicrobial Agents and Chemotherapy*, 55(3):1045-1052.
- Meinhardt SW, Crofts AR. 1982. The site and mechanism of action of myxothiazol as an inhibitor of electron transfer in *Rhodopseudomonas sphaeroides*. *FEBS Letters*, 149(2):217-222.
- Mookerjee SA, Goncalves RLS, Gerencser AA, Nicholls DG, Brand MD. 2015. The contributions of respiration and glycolysis to extracellular acid production. *Biochimica et Biophysica Acta*, 1847(2):171-181.
- Mondal S, Roy JJ, Bera T. 2014. Characterization of mitochondrial bioenergetic functions between two forms of *Leishmania donovani* – a comparative analysis. *Journal of Bioenergetics and Biomembranes*, 46(5):395–402.
- Monzote L, Geroldinger G, Tonner M, Scull R, De Sarkar S, Bergmann S, Bacher M, Staniek K, Chatterjee M, Rosenau T, Gille L. 2018. Interaction of ascaridole, carvacrol, and caryophyllene oxide from essential oil of *Chenopodium ambrosioides* L. with mitochondria in *Leishmania* and other eukaryotes. *Phytotherapy Research*, 32(9):1729-1740.
- Rosenzweig D, Smith D, Opperdoes F, Stern S, Olafson RW, Zilberstein D. 2008. Retooling *Leishmania* metabolism: From sand fly gut to human macrophage. *The FASEB Journal*, 22(2):590–602.
- Sakata-Kato T, Wirth DF. 2016. A novel methodology for bioenergetic analysis of *Plasmodium falciparum* reveals a glucose-regulated metabolic shift and enables mode of action analyses of mitochondrial inhibitors. *ACS Infectious Diseases*, 2(12):903-916.
- Santhamma KR, Bhaduri A. 1995. Characterization of the respiratory chain of *Leishmania donovani* promastigotes. *Molecular and Biochemical Parasitology*, 75(1):43–53.
- Saunders EC, Naderer T, Chambers J, Scott M, Landfear SM, McConville MJ. 2018. *Leishmania mexicana* can utilize amino acids as major carbon sources in macrophages but not in animal models. *Molecular Microbiology*, 108(2):143–158.
- Smith RAJ, Hartley RC, Cochemé HM, Murphy MP. 2012. Mitochondrial pharmacology. *Trends in Pharmacological Sciences*, 33(6):341–352.

Taylor VM, Muñoz DL, Cedeño DL, Vélez ID, Jones MA, Robledo SM. 2010. *Leishmania tarentolae*: Utility as an in vitro model for screening of antileishmanial agents. *Experimental Parasitology*, 126(4):471–475.

Wu M, Neilson A, Swift AL, Moran R, Tamagnine J, Parslow D, Armistead S, Lemire K, Orrell J, Teich J, Chomicz S, Ferrick DA. 2007. Multiparameter metabolic analysis reveals a close link between attenuated mitochondrial bioenergetic function and enhanced glycolysis dependency in human tumor cells. *American Journal of Physiology-Cell Physiology*, 292(1):C125-C136.

10 ACKNOWLEDGEMENTS

Above all, I would like to express my sincere thanks to my supervisor Ao. Univ. Prof. Dr. Katrin Staniek, whose expertise was invaluable. I am very grateful for her dedicated guidance, endless support and her worthwhile time from the beginning to the end of this study and also her perpetual encouragement and professional advice.

Furthermore, I would like to express my gratitude to Ao. Univ. Prof. Dr. Lars Gille, for his support, advice and his contributions to this study. Also, I would like to thank his bachelor student Sara Todhe and Laura Machin for their help and effort.

I further owe the whole team of the Institute of Pharmacology and Toxicology my sincere thanks for their assistance and the pleasant working atmosphere, in particular Maria Tutzer, Reimar David, Meryem Şen and Petra Kudweis.

In addition, I would like to thank my family, especially my parents, for their endless encouragement. I could not have completed this thesis without the support of my friends and the interesting discussions with them.